

# Modelling Precipitation and Surface Complexation Reactions in Systems with Goethite, Cu(II) and Oxyanions Containing As(V) or P(V)

**Hanna Nelson**



**Department of Chemistry**  
Umeå 2012

This work is protected by the Swedish Copyright Legislation (Act 1960:729)  
ISBN: 978-91-7459-381-5  
Electronic version available at <http://umu.diva-portal.org/>  
Printed by: KBC-Tryckeriet  
Umeå, Sweden 2012

## Abstract

The aqueous solubility of oxyanion (e.g. phosphates and arsenates), and thereby their mobility, bioavailability (phosphates) and toxicity (arsenates), in soils and sediments is dependent upon their chemical speciation. In complex, multicomponent systems, equilibrium modelling can be a useful tool to predict chemical speciation. When establishing a model, it is essential to understand the interactions between all the components not only in solution but also on mineral surfaces at a molecular level. By applying surface complexation models processes at mineral surfaces can be accounted for.

This thesis is a summary of four papers and focuses on surface complexation of the oxyanions arsenate, phosphate and monomethyl phosphate adsorbed onto the surface of goethite ( $\alpha$ -FeOOH). Furthermore, adsorption and precipitation of copper(II) arsenates from aqueous solutions has been studied.

Solid copper(II) arsenates obtained in precipitation experiments were characterised and five different solid phases with different Cu(II) to As(V) ratio, as well as proton and Na<sup>+</sup> content, were identified;  $\text{Cu}_5\text{Na}(\text{HAsO}_4)(\text{AsO}_4)_3(\text{s})$ ,  $\text{Cu}_5\text{Na}_2(\text{AsO}_4)_4(\text{s})$ ,  $\text{Cu}_3(\text{AsO}_4)_2(\text{s})$ ,  $\text{Cu}_3(\text{AsO}_4)(\text{OH})_3(\text{s})$  and  $\text{Cu}_2(\text{AsO}_4)(\text{OH})(\text{s})$ . The adsorption of arsenate and copper(II) to the goethite surface, could not be predicted by only applying the combined model from the two binary systems, arsenate-goethite and copper(II)-goethite. Instead, two ternary copper-arsenate-goethite surface complexes were added. In one of the surface complexes arsenate is bound to goethite surface via a copper(II) ion coordinating to surface hydroxyl groups and in the other surface complex, copper(II) is coordinating arsenate bound to the goethite surface.

Surface complexation models, in agreement with macroscopic data and detailed spectroscopic results, were designed for monomethyl phosphate, phosphate and arsenate adsorbed to goethite. The models contain monodentate inner sphere surface complexes stabilized by hydrogen bonding to neighbouring surface sites. The charge distribution of the complexes was assigned according to Pauling's valence bond theory.

The monomethyl phosphate model consists of three singly protonated surface isomers, only differentiated by the location of the proton. In the case of phosphate and arsenate, six surface complexes, including two pair-wise surface isomers, are suggested to form;  $\equiv\text{FeOAsO}_3^{2.5-}$ ;  $(\equiv\text{FeOAsO}_3; \equiv\text{Fe}_3\text{OH})^{2-}$ ;  $(\equiv\text{FeOAsO}_3\text{H}; \equiv\text{Fe}_3\text{O})^{2-}$ ;  $(\equiv\text{FeOAsO}_3\text{H}; \equiv\text{Fe}_3\text{OH})^{1-}$ ;  $(\equiv\text{FeOAsO}_3\text{H}_2; \equiv\text{Fe}_3\text{O})^{1-}$  and  $\equiv\text{FeOAsO}_3\text{H}_2^{0.5-}$ . A combination of structural information from spectroscopic measurements and quantitative data from spectroscopy, potentiometry and adsorption experiments provides a better understanding of the complexity of the coordination chemistry of particle surfaces and forms the basis for equilibrium models with high physical/chemical relevance.

Modelling Precipitation and Surface Complexation Reactions  
in Systems with Goethite, Cu(II) and Oxyanions Containing  
As(V) or P(V)

Hanna Nelson

This thesis contains a summary and a discussion of the following papers, referred to in  
the text by their Roman numerals I-IV

- I      **Composition and Solubility of Precipitated Copper(II) Arsenates**  
Hanna Nelson, Andrey Shchukarev, Staffan Sjöberg, Lars Lövgren  
*Applied Geochemistry, 2011, (26), 696-704*  
Reprinted with permission from Elsevier
- II     **Surface Complexation Modelling of Arsenate and Copper(II) Adsorbed at  
the Goethite/ Water Interface**  
Hanna Nelson, Staffan Sjöberg and Lars Lövgren  
Submitted to Applied Geochemistry
- III    **Surface Complexes of Monomethyl Phosphate Stabilized by Hydrogen  
Bonding on Goethite ( $\alpha$ -FeOOH) Nanoparticles**  
Per Persson, Tove Andersson, Hanna Nelson, Staffan Sjöberg, Reiner Giesler and Lars Lövgren  
Submitted to Journal of Colloid and Interface Science
- IV    **Monodentate Inner-Sphere Coordination of Arsenate and Phosphate  
Anions, Stabilized by Hydrogen Bonding, at the Goethite/Water Interface**  
Hanna Nelson, Staffan Sjöberg and Lars Lövgren  
Manuscript

## CONTENTS

1.	Introduction.....	1
2.	Aim .....	2
3.	Solutions, Solids and Surfaces .....	3
3.1.	Complexation in Solution.....	3
3.2.	Solid Phases.....	4
3.2.1.	<i>Copper(II)-Arsenates</i> .....	4
3.3.	The Goethite Surface.....	4
3.3.1.	<i>Copper(II)-Goethite</i> .....	5
3.3.2.	<i>Copper(II)-Arsenate-Goethite</i> .....	5
3.3.3.	<i>Arsenate-, Phosphate-, Monomethyl Phosphate- Goethite</i> .....	5
4.	Experimental Procedures.....	7
4.1.	Goethite .....	7
4.2.	Potentiometric Titrations.....	7
4.3.	Batch Adsorption Experiments .....	8
5.	Equilibrium Modelling.....	9
5.1.	Surface Complexation Models.....	9
5.1.1.	<i>The Basic Stern Model</i> .....	9
5.1.2.	<i>Charge Distribution</i> .....	10
5.2.	Complexation at the Goethite Surface .....	11
6.	Data Treatment .....	13
7.	Results.....	15
7.1.	Composition and Solubility of Precipitated Copper(II) Arsenates .....	15
7.1.1.	<i>Protonation Equilibria of <math>\text{HAsO}_4^{2-}</math></i> .....	15
7.1.2.	<i>Copper(II) complexation with <math>\text{HAsO}_4^{2-}</math></i> .....	15
7.1.3.	<i>Copper(II) Precipitation with <math>\text{HAsO}_4^{2-}</math></i> .....	15
7.2.	Complexation of Arsenate and Copper(II) at the Goethite/ Water Interface .....	19
7.2.1.	<i>Arsenate Complexation</i> .....	19
7.2.2.	<i>Copper(II) Complexation</i> .....	20
7.2.3.	<i>Arsenate-Copper(II) Complexation</i> .....	21
7.3.	Complexation of Monomethyl Phosphate, Phosphate and Arsenate at the Goethite/ Water Interface.....	24
7.3.1.	<i>Complexation of Monomethyl Phosphate</i> .....	26
7.3.2.	<i>Complexation of Phosphate</i> .....	27
7.3.3.	<i>Complexation of Arsenate</i> .....	29
8.	Summary and Conclusions .....	31
9.	References.....	33
	Acknowledgements .....	36

## 1. Introduction

Arsenic is an element of great environmental significance, since high levels of arsenic in groundwater are a severe threat to public health in many parts of the world. The source of the high arsenic concentrations is primarily due to natural occurrences of arsenic in soils and bedrock. A sharp increase in exposure observed during the last decades can, however, largely be attributed to recent human activities, such as extraction of groundwater from increasingly greater depths. In Europe, while arsenic contamination is commonly related to human activities related to mining, it also stems from spills from wood preservation techniques, which used fluids containing copper, chromium and arsenic.

In natural oxidised waters, arsenic is mostly found in inorganic form as the oxyanion arsenate,  $\text{AsO}_4^{3-}$ . Arsenate can react with metal ions in the solution and form soluble complexes. Arsenate can also precipitate and form solid metal arsenates. Even if the arsenate does not react directly with the other components in the solution, adsorption of these other components to mineral surfaces can affect the arsenate adsorption. The arsenate adsorption can be increased or decreased depending on the nature of the surfaces and the other adsorbed components.

An oxyanion with similar physicochemical properties as arsenate is phosphate. Unlike the toxic arsenic, phosphorus is an essential element to all known forms of life. Phosphorus is often a limiting factor for plant growth, since the bioavailable phosphorus species, phosphate, only makes up a minor fraction of the total phosphorus in soils and sediments. The larger fraction of phosphorus is retained in the soils by sorption to soil particles, by precipitation with metal ions or incorporated into soil organic matter. [1] Additionally, a substantial part of the total phosphorus in soils consists of organophosphates, like monomethyl phosphate, which makes them an important potential phosphorus source for organisms [2].

The aqueous solubility, and thereby the mobility and bioavailability, of oxyanions in soils and sediments is generally considered to be limited by adsorption to particle surfaces [3]. However, it is important to consider all possible reactions that may affect their solubility, which includes not only adsorption processes but also precipitation/dissolution of solid phases, protonation/ deprotonation of aqueous species and formation of metal complexes in solution.

To assess the risks associated with arsenic contamination, and to design remediation measures in cases of strongly contaminated sites, or to design efficient fertilisers in the case of phosphate, it is of critical importance to understand the geochemistry of these

anions and their interaction with geologic materials. A keyword in this sense is speciation, i.e. the distribution of the ion between different chemical forms.

In complex, competitive, multicomponent systems, surface complexation modelling can be a useful tool to predict speciation. When establishing a model, it is essential to understand the interactions between all the components in solution and on the mineral surfaces at a molecular level. By basing the model on a combination of quantitative data and structural characterizations from spectroscopic methods, this model can predict the speciation both in solution and at mineral surfaces and would be valid at a range of chemical conditions.

## 2. Aim

The aim of this thesis is to contribute to the understanding of the geochemistry of oxyanions and their interaction with geologic materials. In order to understand their mobility and bioavailability, the aqueous speciation of oxyanions needs to be further studied. This was accomplished by studying equilibrium reactions in binary systems including goethite together with the oxyanions; arsenate, phosphate or monomethyl phosphate. Furthermore, the ternary system copper(II)-arsenate-goethite was studied to investigate the impact of a metal ion on the solubility of oxyanions in these systems.

An important tool for understanding oxyanion mobility and bioavailability is equilibrium modelling. Therefore, to fulfil the aim of this thesis, new models that are consistent with spectroscopic data for the investigated systems have been developed.

### 3. Solutions, Solids and Surfaces

A prerequisite for successful modelling of geochemical processes, e.g. in soils, is access to consistent sets of model parameters, including all types of chemical equilibria involved. It is of critical importance to be able to consider formation of possible soluble complexes and solid species, as well as formation of surface complexes on mineral particles (Figure 3.1). As an example, the equilibrium model for the system  $\text{H}^+$ - $\text{HAsO}_4^{2-}$ - $\text{Cu}^{2+}$ - goethite includes; hydrolysis of  $\text{Cu}^{2+}$ , protonation/ deprotonation of the hydrogen arsenate ion and the goethite surface, possible complexation of  $\text{Cu}^{2+}$  and arsenate in solution, formation of solid copper(II) (hydr)oxide and copper(II) arsenates, complexation of  $\text{Cu}^{2+}$  and arsenate, separately, and  $\text{Cu}^{2+}$  and arsenate together at the goethite surface.

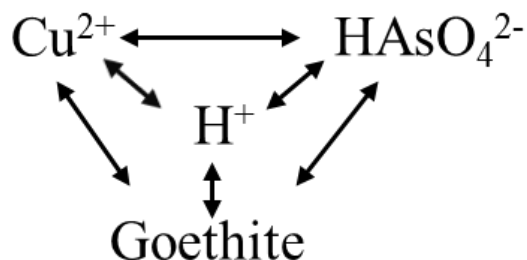


Figure 3.1. Cartoon of the components and equilibria that have to be taken into account when modelling a the ternary system copper(II)-arsenate-goethite.

To significantly improve the quality of the model it is of great value to have structural information on molecular level, as obtained from spectroscopic methods like EXAFS and FTIR, available. In the following sections, the available information from the literature about reactions involved in the systems investigated in this thesis is discussed.

#### 3.1. Complexation in Solution

The acid/base properties of arsenate and phosphate are very similar. For instance, the protonation constant ( $\log\beta_{1,1}$ ) of  $\text{HAsO}_4^{2-}$  in 0 M ionic strength is 7.13 [4] and the corresponding value for phosphate is 7.20 [5]. Monomethyl phosphoric acid is a diprotic acid with one pKa value at low pH and the second at 6.71 (I=0 M) which is the only one to consider in the pH region studied here. [6]. Also Cu(II) can be considered as a weak acid. Hydrolysis of  $\text{Cu}^{2+}$  ions, which includes both formation of hydroxide complexes in aqueous solution and precipitation of Cu(II) hydroxides and oxides, generates protons which are released to the solution [7].

Considering possible soluble copper-arsenate complexes, only two studies, by Marini and Accornero [8] and Lee and Nriagu [9], were found in IUPAC's stability constants database [10]. Based on a theoretical approach, Marini and Accornero [8] predicted formation constants of aqueous metal-arsenate complexes, including three different



complexes with a copper to arsenate ratio of one, i.e.  $\text{CuH}_2\text{AsO}_4^+$ ,  $\text{CuHAsO}_4^0$  and  $\text{CuAsO}_4^-$ . In an experimental investigation of the solubility product of metal arsenate complexes, Lee and Nriagu [9] made an attempt using ion chromatography to identify aqueous metal-arsenate complexes. For Cu(II) no such complexes could be found at pH 3.6, which was the only pH investigated.

### 3.2. Solid Phases

#### 3.2.1. Copper(II)–Arsenates

The literature on metal arsenate species is limited, both for soluble complexes and solid phases. Magalhães et al. [11] studied the dissolution of a set of metal arsenate minerals with copper to arsenate ratios ranging from 2 to 3. The copper minerals studied were olivenite [ $\text{Cu}_2(\text{AsO}_4)(\text{OH})$ ], cornubite [ $\text{Cu}_5(\text{AsO}_4)_2(\text{OH})_4$ ] and clinoclase [ $\text{Cu}_3\text{AsO}_4(\text{OH})_3$ ]. Besides this study, Lee and Nriagu [9] and Chukhlantsev [12] have determined the solubility product of  $\text{Cu}_3(\text{AsO}_4)_2$ .

### 3.3. The Goethite Surface

Goethite is an iron oxyhydroxide consisting of oxygen octahedra with trivalent iron ions in the middle. The main crystal plane of the needle shaped goethite particles is the  $\{110\}$  plane. This plane represents more than 90 % of the total surface area [13]. The  $\{110\}$  plane exhibits singly- ( $\equiv\text{FeOH}^{-0.5}$ ), doubly- ( $\equiv\text{Fe}_2\text{OH}^0$ ), and triply-coordinated ( $\equiv\text{Fe}_3\text{O}^{-0.5}$ ) oxygens in rows along the  $\{001\}$  axis (Figure 3.2) [14]. The crystallographic density of singly- and triply-coordinated surface sites are 3.56 and 2.81 sites/ $\text{nm}^2$  respectively [15], which gives a total concentration of proton active sites of  $6.37 \mu\text{mol}/\text{m}^2$ .

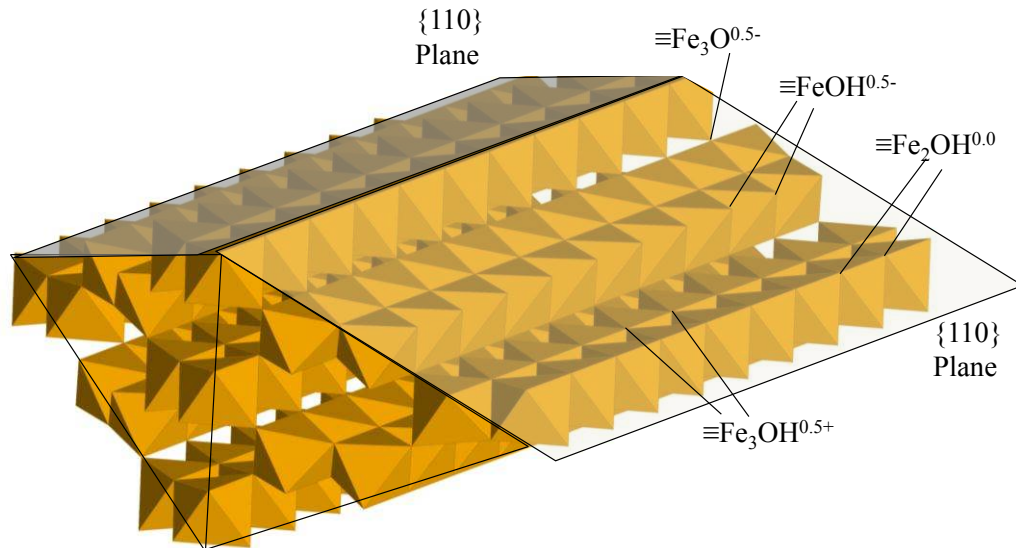


Figure 3.2. Schematic representation of the  $\{110\}$  plane of the goethite particle. Modified from [16].

### 3.3.1. *Copper(II)-Goethite*

It has been shown using EXAFS that copper(II) can form inner-sphere complexes at the edges of the goethite particles. Hydroxo-bridged polymeric copper(II) species are most likely formed [17]. These polymeric species has been modeled previously with a range of surface complexes, including polymeric species [18], [19]. Weng et al. [20] suggested a model consisting of four bidentate complexes, two mononuclear species ( $(\equiv\text{FeOH})_2\text{Cu}^{1+}$  and  $(\equiv\text{FeOH})_2\text{Cu}(\text{OH})^0$ ), and two binuclear species ( $(\equiv\text{FeOH})_2\text{Cu}_2(\text{OH})_2^{1+}$  and  $(\equiv\text{FeOH})_2\text{Cu}_2(\text{OH})_3^0$ ). Recently Heimstra [21] proposed the copper atom to be coordinated by one singly and one triply coordinated surface site ( $(\equiv(\text{Fe}_3\text{OFeOH})\text{CuOH})^0$ ).

### 3.3.2. *Copper(II)-Arsenate-Goethite*

Gräfe and co-workers have published two EXAFS studies on the co-adsorption of copper(II) and arsenate onto the surface of goethite. In the first paper, the bonding environment of arsenate on goethite and gibbsite in the presence of Cu(II) and Zn(II) was studied at pH 7.0 [22]. From this data the second nearest Cu(II) neighbors could not be ascertained unambiguously for the goethite samples. However, on gibbsite  $\text{AsO}_4$  bonding with polymeric Cu species at the gibbsite surface appeared to take place. In the second paper, Gräfe et al. [23], found evidence for a hydrated clinoclase- like  $(\text{Cu}_3\text{AsO}_4(\text{OH})_3$  (s)) copper-arsenate precipitate at the goethite surface at pH 5.65 and Cu(II) to As(V) ratios greater than 5:1. Khaodhiar et al. [24] modelled the co-adsorption of copper and arsenate at the surface of iron-oxide-coated sand and concluded that the equilibrium constants from the binary systems were not able to predict the adsorption in the ternary system.

### 3.3.3. *Arsenate-, Phosphate-, Monomethyl Phosphate- Goethite*

Oxyanions like arsenate and phosphate has been studied with different spectroscopic methods. The overall conclusion, until recently, was that arsenate and phosphate mainly binds in an inner-sphere bidentate bridging mode to singly coordinated surface sites [25-29]. However, Loring et al. [30], showed that results from arsenate-goethite EXAFS analysis are better interpreted as caused by the formation of monodentate surface complexes. Based on a combination of EXAFS and IR spectroscopy they concluded that arsenate coordinates predominantly in a monodentate fashion to singly coordinated hydroxyl groups on the goethite surface and is stabilized by hydrogen bonding to neighboring surface sites. Loring et al. suggested three major surface complexes dominating at different pH. Two of these complexes are surface isomers, i. e. assigned the same overall stoichiometry but with different protons geometries in the hydrogen bond. At  $\text{pH} > 10$  an unprotonated (with respect to As(V)) complex was identified with the tentative structure,  $(\equiv\text{FeOAsO}_3; \equiv\text{FeOH}_2)^{2-}$ . At  $\text{pH} \approx 6.5$  a complex was suggested where the proton is bound to the adsorbed arsenate ion instead of to the neighboring hydroxyl group,  $(\equiv\text{FeOAsO}_3\text{H}; \equiv\text{FeOH})^{2-}$ . Finally, at  $\text{pH} \leq 3$  a doubly protonated complex,  $(\equiv\text{FeOAsO}_3\text{H}_2; \equiv\text{FeOH})^{1-}$  was suggested. However, from the results presented by Loring

et. al [30] it is not possible to determine if the oxygen of the neighboring site is singly, doubly or triply coordinated with respect to Fe and whether the proton is located closer to the arsenate group or at the neighboring surface site.

Persson et al. [6] drew similar conclusions in the monomethyl phosphate system. Using IR spectroscopy, three monodentate surface complexes hydrogen bonded to a neighbouring surface site were detected; one singly protonated complex hydrogen bonded to a unprotonated neighboring site dominating at pH <6, one complex where the proton is located between the ligand and the neighbouring site dominating at pH 6-8 and one unprotonated surface complex hydrogen bonded to a protonated neighboring surface site dominating at pH >8

The adsorption of arsenate or phosphate to the goethite surface has by several authors been modeled by formation of bidentate bridging surface complexes [31-33].

Monodentate surface complexes have also been presented for arsenate [34, 35]. Recently Salazar-Camacho and Villalobos [36] modeled the adsorption with a monodentate complex at singly coordinated surface sites and hydrogen bonded to neighboring singly or doubly coordinated sites.

## 4. Experimental Procedures

### 4.1. Goethite

Goethite was synthesized as described by Hiemstra et. al [37]. Briefly, NaOH was added to a 0.5 M Fe(III) solution at a slow rate. The suspension was stirred with a propeller at room temperature. The precipitate was aged for 100 h at 60 °C and then dialyzed for two weeks to remove dissolved counter ions and excess hydroxide. The resulting particles were identified to be goethite using X-ray powder diffraction and the surface area was determined using the BET N<sub>2</sub> adsorption method {Brunauer, 1938 #42}. A stock suspension (10 g/L of goethite; 0.1 M NaCl) was adjusted to pH 4.3 and bubbled with nitrogen to remove carbonate adsorbed at the goethite surface and any dissolved CO<sub>2</sub> in solution.

### 4.2. Potentiometric Titrations

Potentiometric titrations were conducted to characterize any possible aqueous complexes in the copper arsenate system and to determine the protonation constants for HAsO<sub>4</sub><sup>2-</sup> (Paper I). Potentiometric titrations were also used to study the acid/base reactions at the goethite surface in the presence of arsenate and/ or copper(II) (Paper II), monomethyl phosphate (Paper III) and phosphate (Paper IV). Furthermore, potentiometric titrations were used to determine the concentration of the stock solution of arsenate and phosphate.

Automated potentiometric titrations were performed according to Ginstrup, [38]. The atmosphere in the closed titration vessel was kept inert by a constant flow of N<sub>2</sub> (g), and the temperature was kept constant at 25 ± 0.1 °C.

The free proton concentration in solution was determined using both a glass and an Ag/AgCl reference electrode. The EMF of the cell was measured and the free proton concentration was calculated according to:

$$E = E_0 + g \log[H^+] + E_j \quad (1)$$

$E_0$  is an apparatus constant for the cell determined by calibration in solutions with known proton concentration and 0.1 M NaCl. The constant  $g$  is equal to 59.16 mV at 25 °C.  $E_j$  is the liquid junction potential between the solution and the salt bridge.

The potentiometric titrations of arsenate, phosphate and monomethyl phosphate adsorbed onto the goethite surface were performed utilizing the SIPT- technique (Simultaneous Infrared Potentiometric Titration) where an infrared spectrum was recorded at every titration point [30].

### 4.3. Batch Adsorption Experiments

Batch adsorption experiments were conducted to quantitatively study the adsorption of copper, arsenate and phosphate at the goethite surface. The experiments were performed in a glove box under nitrogen atmosphere.

A volume of ligand solution was added to the goethite suspension to bring the total ligand concentration in the suspension to the desired concentration, and then the suspension was titrated and volumes of suspension were collected at desired pH. The arsenate, or phosphate, solution was added to the goethite suspension at pH 10 and the copper solution was added at pH 3. In the copper(II)-arsenate-goethite system, copper(II) and arsenate were added simultaneously at pH 6. A previous test series concluded that the order of copper(II) and arsenate addition, or initial pH, had no effect on the equilibrium concentrations.

The concentrations of As(V) and P(V) were analysed by ion chromatography (IC). Atomic absorption spectrometry (AAS) was used to analyse the concentration of copper(II) in the supernatant. AAS was also used to detect any iron that may have been present due to dissolution of goethite. The concentrations of monomethyl phosphate in solution were analysed colorimetrically with the ammonium molybdate method [39].

## 5. Equilibrium Modelling

In complex, competitive, multicomponent systems, equilibrium modelling can be a useful tool to predict speciation in solution and at particle surfaces as well as the formation of solid phases. The models are valid at any pH and reactant concentrations, provided that the models are established using an extensive set of experimental data.

### 5.1. Surface Complexation Models

Surface complexation models (SCM) are used to describe equilibrium reactions at the mineral surface/ water interface. The formation of surface complexes can be described by mass law equations in a similar way as complexation reactions in solution. The formation constants for surface complexes must, however, be corrected for the electrostatic effects that are built up at the surface when protons and charged ligands are adsorbed. The charge dependent formation constant for a surface complex, the apparent formation constant ( $\beta_{app}$ ), is the product of the intrinsic constant ( $\beta_{intr}$ ) that is valid for an uncharged surface and a correction term for electrostatic effects.

$$\beta_{app} = \beta_{intr} \sum_{i=1}^N e^{\left(-\frac{\Delta z_i \psi_i F}{RT}\right)} \quad (2)$$

where N is the number of planes at which charges are assumed to be located, and this is dependent on which SCM that is applied.  $\Delta z_i$  is the difference in charge between the formed and reacting surface species at the  $i^{\text{th}}$ - plane, and  $\psi_i$  is the potential at this plane.

#### 5.1.1. The Basic Stern Model

In this thesis the Basic Stern Model (BSM) is used to correct for electrostatic forces due to adsorption of charged ions. The BSM is one of the simplest models that accounts for ionic strength dependence and it is valid over a broad range of ionic strengths. The electrostatic double layer consists of an inner compact layer and a diffuse layer of counter ions, the charge of the surface complexes can be placed either at the surface plane (0-plane) or at the plane that separates the inner plane from the diffuse layer ( $\beta$ -plane) (Figure 5.1). The surface charge is related to the surface potential according to the Gouy-Chapman theory [40]. The surface potential of the diffuse layer decreases to zero with distance to the surface. Electroneutrality of the interface is defined by:

$$\sigma_0 + \sigma_\beta + \sigma_{dl} = 0 \quad (3)$$

where  $\sigma_0$ ,  $\sigma_\beta$  and  $\sigma_{dl}$  are the charge densities at the 0-plane, the  $\beta$ -plane and in the diffuse layer, respectively. The values of the potentials,  $\psi_0$  and  $\psi_\beta$ , are calculated according to:

$$\psi_0 - \psi_\beta = \frac{\sigma_0}{C_{Stern}} \quad (4)$$

where  $C_{Stern}$  is the capacitance of the charge-free Stern layer, located between the 0-plane and the  $\beta$ -plane.

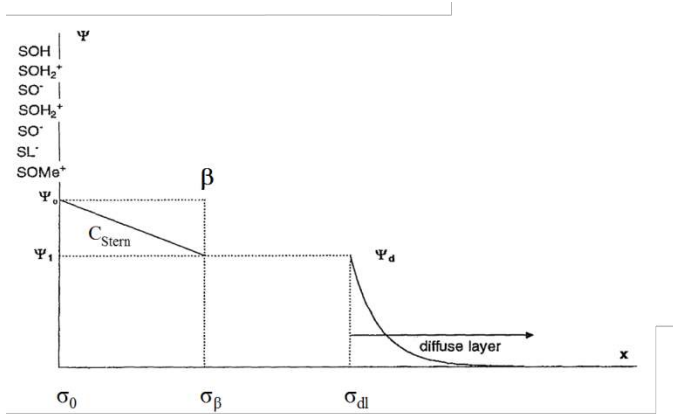


Figure 5.1. Schematic representation of the water-surface interface according to the Basic Stern Model. The potential ( $\Psi$ ) as a function of distance from the surface ( $x$ ). Modified from [41].

### 5.1.2. Charge Distribution

In this concept of charge distribution, the charge of the surface complex is distributed over the 0-plane and the  $\beta$ -plane. A fraction of the total charge is located at the 0-plane and the other fraction is assigned to the  $\beta$ -plane. The charge of the 0-plane and the  $\beta$ -plane are denoted  $Q_0$  and  $Q_\beta$ , respectively. The distribution of the charge between  $Q_0$  and  $Q_\beta$  can be optimized but often the values of  $Q_0$  and  $Q_\beta$  are assumed using Pauling's bond valance theory.

The charge of the surface sites is determined by the coordination mode of the metal in the crystal structure and is based on Pauling's bond valance theory [43]. Assuming that the charge is distributed symmetrically over surrounding bonds, a formal bond valance ( $v$ ) can be defined as:

$$v = \frac{z}{CN} \quad (5)$$

where  $Z$  is the charge of the metal ion and  $CN$  is the coordination number. With regard to goethite, the charge of the iron is neutralized by six oxygen atoms, leading to a formal charge of +0.5 at each bond. The charge of the surface (hydr)oxyl, is partly neutralised by the iron- oxygen bond which gives that the charge of the unprotonated singly- and triply coordinated surface sites are -0.5 and the doubly coordinated sites are neutral.

In a monodentately coordinated arsenate ion, the surface oxygen is partly neutralised by the iron-oxygen bond, and partly by the arsenate- oxygen bond. The As(V) ion is coordinated to four oxygen atoms, leading to a formal charge of 1.25 at each bond. The charge of the surface oxygen is -0.25 ( $0.5 - 2 + 1.25 = -0.25$ ), and this fraction of the total charge of the surface complex is assigned to the 0-plane

If a monodentately adsorbed arsenate acts as a hydrogen bond donor in a surface complex stabilised by hydrogen bonding to a neighbouring site, the charge in the 0-plane for the complex is -0.75. If the neighbouring site acts as the hydrogen donor, the charge in the 0-plane is 0.25.

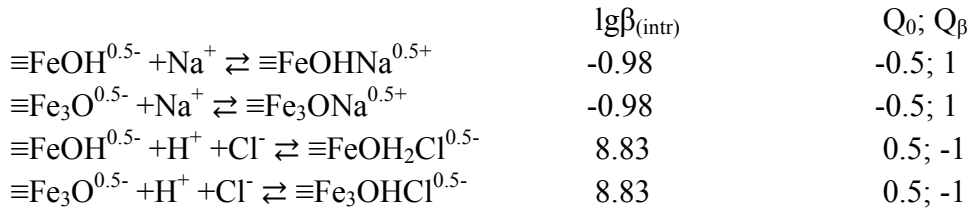
## 5.2. Complexation at the Goethite Surface

The heterogeneity of the goethite surface is addressed using the MUSIC model developed by Hiemstra and co-workers [37, 42], which uses crystallographic information to distinguish singly-, doubly-, and triply coordinated O(H) and OH(H) surface groups of (hydr)oxide minerals.

The singly-coordinated,  $\equiv\text{FeOH}^{0.5-}$  and the triply-coordinated  $\equiv\text{Fe}_3\text{O}^{0.5-}$  are considered to be responsible for the reactivity of the goethite surface in the pH range 1-11 [44]. Based on crystallographic data for goethite the site densities of singly- and triply- coordinated surface sites are 3.56 and 2.81 sites/nm<sup>2</sup> respectively [15]. Protonation reactions, protonation constants, and charge distribution over the 0-plane and the  $\beta$ -plane for the singly- and triply-coordinated surface sites are:



Charged ions from the ionic media act as counter ions in the diffuse layer but they also interact with the oppositely charged surface sites. In the models presented in this thesis surface complexes involving  $\text{Na}^+$  and  $\text{Cl}^-$  ions have been included [15].



Looking at the goethite surface, the singly coordinated surface sites adsorbing ligands are close enough to both other singly coordinated sites and triply coordinated sites to form bidentate surface complexes or in the case of monodentate complexes form hydrogen bonds to neighbouring sites (Figure 5.2). Under the chemical conditions applied in this thesis, with total concentrations of ligands lower than the total number of singly coordinated surface sites, modelling was not a tool to determine if the ligands coordinate to singly or triply coordinated surface sites.



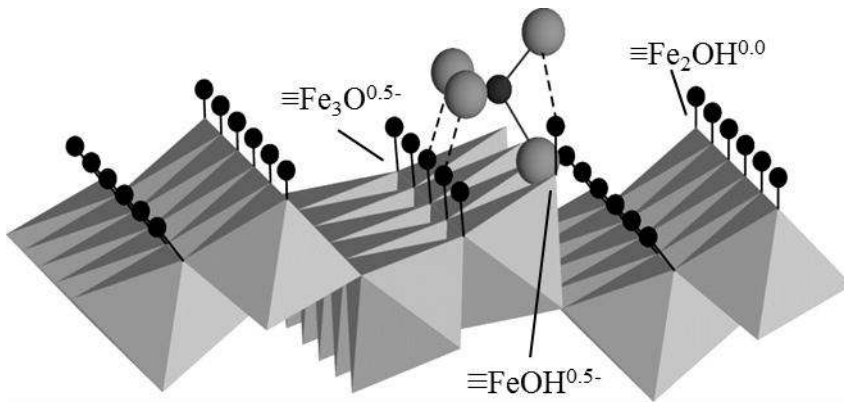
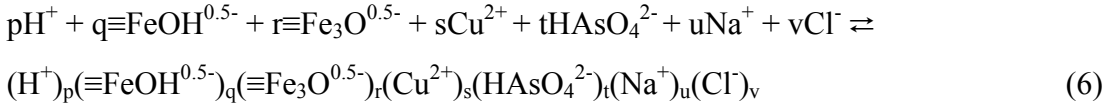


Figure 5.2. Section of the {110} plane of the goethite surface. An arsenate atom is adsorbed in a monodentate fashion to a singly coordinated surface site to illustrate the possibility of hydrogen bonding to a neighbouring singly- or triply coordinated surface site.

By assigning the coordination of adsorbed ligands to one singly and one triply coordinated surface site, the problem of expressing the law of mass action with regard to representation of the concentration of surface sites in complexes involving two sites of the same type can be avoided. According to the law of mass action the exponent in such cases should be 2. This exponent reflects the probability that two surface sites of the same type are brought together in one complex. However, when dealing with surface complexes the two sites must be neighbours. Hence, the probability term, i.e. the exponent, should be lower than 2.

## 6. Data Treatment

The ternary system copper(II)- arsenate- goethite is used as an example of the equilibrium analysis performed in this thesis. The following reacting components are present in this system:  $H^+$ ,  $\equiv FeOH^{0.5-}$ ,  $\equiv Fe_3O^{0.5-}$ ,  $Cu^{2+}$ ,  $HAsO_4^{2-}$ ,  $Na^+$  and  $Cl^-$ . A general equilibrium reaction for the formation of soluble complexes, solid phases and surface complexes can be written as:



This general reaction defines the equilibrium constant  $\beta_{p,q,r,s,t,u,v}$ .

The total concentration of each component ( $C(tc)$ ) is given by its total concentration in solution ( $C(sln)$ ), its amount in the solid phases per  $dm^3$  solution ( $n(sld)$ ) and its total concentration at the surface ( $C(srfc)$ ):

$$C(tc) = C(sln) + n(sld) + C(srfc) \quad (7)$$

The  $C(tc)$  of each chemical component is obtained by summing the products of the concentration of each aqueous, solid and surface species times the stoichiometric coefficient of the component in each species. For example, the total concentration of protons ( $H$ ) is given by the following equation:

$$H(tc) = H(sln) + H(sld) + H(srfc) = [H^+] - [OH^-] - [CuOH^+] - 2[Cu(OH)_2(aq)] - \dots - [AsO_4^{3-}] + [H_2AsO_4^-] + 2[H_3AsO_4] + \dots - 3n(Cu_5Na(HAsO_4)(AsO_4)_3(s)) - \dots + [\equiv FeOH_2^{0.5+}] + \dots + 2[(\equiv FeOAsO_3; \equiv Fe_3OH_2)^-] - [(\equiv Fe_3OFeOH)Cu(OH)^0] - \dots \quad (8)$$

The computer code WinSGW, [45] based on the SOLGASWATER algorithm [46] was used to fit the equilibrium model to the experimental data. WinSGW minimizes on the total residual sum of squares ( $U$ ), calculated from the total proton concentration ( $U_{H(tc)}$ ) and the concentration of copper(II) and arsenate in solution ( $U_{Cu(sln)}$  and  $U_{As(sln)}$ ).

$$U = U_{H(tc)} + U_{Cu(sln)} + U_{As(sln)} \quad (9)$$

The total proton concentrations were analyzed by minimizing the following sum of squares of the deviations:

$$U_{H(tc)} = \sum_{i=1}^N (H(tc)_{i,calc} - H(tc)_{i,exp})^2 \quad (10)$$

here  $H(tc)_{i,calc}$  and  $H(tc)_{i,exp}$  are the calculated and experimental total proton concentrations, respectively, for the  $i^{th}$  data point and  $N$  is the overall number of data

points.  $H(tc)_{i,exp}$  values were obtained from the potentiometric titration data and the batch experiments.

Similarly, adsorption data were treated according to:

$$U_{Cu(sln)} = \sum_{i=1}^N (Cu(sln)_{i,calc} - Cu(sln)_{i,exp})^2 \quad (11)$$

$$U_{As(sln)} = \sum_{i=1}^N (As(sln)_{i,calc} - As(sln)_{i,exp})^2 \quad (12)$$

with  $Cu(sln)_{i,exp}$  and  $As(sln)_{i,exp}$  obtained from the batch experiments.

The Davies equation [47], equation 13, was applied to adjust activity coefficients in the extrapolation of constants to  $I= 0.1$  M.

$$\text{Log } \gamma_i = -0.509z_i^2 \cdot \left( \frac{\sqrt{I}}{1 + \sqrt{I}} - 0.2I \right) \quad (13)$$

$\gamma_i$  is the activity coefficient for the  $i^{\text{th}}$  species,  $z_i$  is the charge of the species and  $I$  is the ionic strength in molar. The Davies equation was used because it represents the data best at the ionic strength of 0.1 M [40].

The results of the potentiometric titrations are visualized as  $Z_H$ - curves.  $Z_H$  is defined as the average number of protons bound per surface site, and is calculated according to Equation 14.

$$Z_H = (H(tc) - [H^+] + [OH^-]) / ([\equiv FeOH^{0.5-}] + [\equiv Fe_3OH^{0.5-}])(tc) \quad (14)$$

## 7. Results

### 7.1. Composition and Solubility of Precipitated Copper(II) Arsenates

The aqueous solubility of arsenic in soils and sediments is generally considered to be limited by the adsorption of arsenic anions to particle surfaces, rather than by dissolution/precipitation of arsenic containing solid phases [3]. However, to be able to distinguish between precipitation and/or adsorption reactions, composition and stability of the solid phases must be known. When the solubility product of copper(II) arsenate in water is to be determined, it is of critical importance to be able to correct for the formation of protonated arsenate species as well as the possible formation of soluble Cu(II) arsenate complexes.

The objectives of the study in Paper I were to determine i) the protonation constants for  $\text{HAsO}_4^{2-}$ , ii) possible complexation between Cu(II) and As(V) in solution and iii) composition and solubility of precipitates formed in Cu(II) - As(V) solutions.

#### 7.1.1. Protonation Equilibria of $\text{HAsO}_4^{2-}$

The protonation constants for  $\text{HAsO}_4^{2-}$  were determined and the following values were obtained (25° C, I= 0.1 M NaCl):



These constants implies that  $\text{p}K_a(\text{H}_3\text{AsO}_4) \equiv \log K_3 = 2.25$ . An extrapolation to zero ionic strength (using Davies equation) of the two protonation constants given above, results in  $\log K_2^0 = 7.13$  and  $\log(K_2 \cdot K_3)^0 = 9.61$ . This also implies that  $\text{p}K_a^0(\text{H}_3\text{AsO}_4) = 2.48$ . This value is about 0.2 log units higher than those found in the IUPAC Stability Constants [10] (25°, I= 0 M). A linear regression analysis of data for  $\log K_3$  from the database, has been performed and the regression yields the value  $\log K_3^0 = 2.48 \pm 0.01$ . This value is in excellent agreement with the value obtained in the present study.

#### 7.1.2. Copper(II) complexation with $\text{HAsO}_4^{2-}$

No evidence of any soluble copper(II) arsenate complexes were found in the pH range studied. Potentiometric titrations of pure arsenate solution and solutions with different copper to arsenate ratios were performed, and the titration curve for As(V) in solution remained unaffected by the presence of copper at pH below 4, regardless of Cu(tc) and As(tc). Precipitates formed at pH > 4.

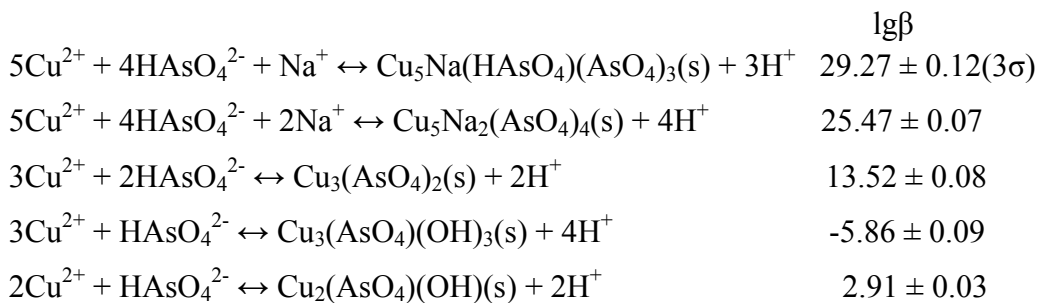
#### 7.1.3. Copper(II) Precipitation with $\text{HAsO}_4^{2-}$

The solid phases formed in batch experiments at different pH and at different total concentrations of copper(II) and arsenate were analysed with respect to Cu/As ratio,

basicity and Na<sup>+</sup> and/or Cl<sup>-</sup> content. An average Cu/As ratio can be calculated knowing the difference between experimental Cu(tc) and Cu(sln) and As(tc) and As(sln), respectively, and also by chemical analysis of the different dissolved precipitate. Furthermore, XPS and SEM-EDS analysis provide information about the average Cu/As ratio at the surface. The basicity of the precipitates, i.e. the number of protons released from HAsO<sub>4</sub><sup>2-</sup> (or Cu<sup>2+</sup>) during formation of the solid phase, is calculated as -H(sld)/As(sld) and -H(sld)/Cu(sld), respectively. The results from both the XPS and the SEM measurements give clear evidences that most of the precipitates, except the most alkaline, contain Na<sup>+</sup> ions. The Na/As ratio is obtained after adjustment for the content of chloride ions assuming that all the chloride ions are present in the solid phase in the form of NaCl.

In summary, the present experimental data show formation of precipitates with varying composition with respect to Cu/As ratio, as well as basicity. The SEM and XPS analysis also show the solid phases to contain Na<sup>+</sup> ions. With the average values  $1.25 \leq \text{Cu/As} \leq 3.4$ ;  $0.8 \leq \text{basicity} \leq 4.0$ ; and  $0 \leq \text{Na/As} \leq 0.5$  a great number of phase compositions are possible. As the XRD measurements gave no indication of which phases are present, we assumed that two Na<sup>+</sup> containing phases with the stoichiometric compositions Cu<sub>5</sub>Na(HAsO<sub>4</sub>)(AsO<sub>4</sub>)<sub>4</sub> and Cu<sub>5</sub>Na<sub>2</sub>(AsO<sub>4</sub>)<sub>4</sub> are formed. Both have a Cu/As ratio of 1.25, an As - basicity of 0.75 and 1, respectively, and a Na/As ratio of 0.25 and 0.5. A good candidate for a solid phase with Cu/As = 1.5 is Cu<sub>3</sub>(AsO<sub>4</sub>)<sub>2</sub>, which has a basicity of 1. Furthermore, Cu/As ratios of 2 and 3 with basicities of 2 – 4 seem likely thinking of the mineral given by Magalhães et al. [11]. Phases with the compositions Cu<sub>2</sub>(AsO<sub>4</sub>)(OH), and Cu<sub>3</sub>(AsO<sub>4</sub>)(OH)<sub>3</sub> therefore are likely candidates.

Based on the collective information from the experimental analyses, a model with five solid phases was proposed.



Depending on total concentration of the components, the solid phases are formed within different pH ranges. Diagrams with distribution of the solid phases formed for two different Cu/As ratios are shown in Figure 7.1. The soluble fraction of Cu and As (experimental and calculated) are included as well. These diagrams also show

overlapping pH – ranges, within which the different solid phases are stable. As can be seen in Figure 7.1b, up to three co-existing solid phases are present in some pH ranges.

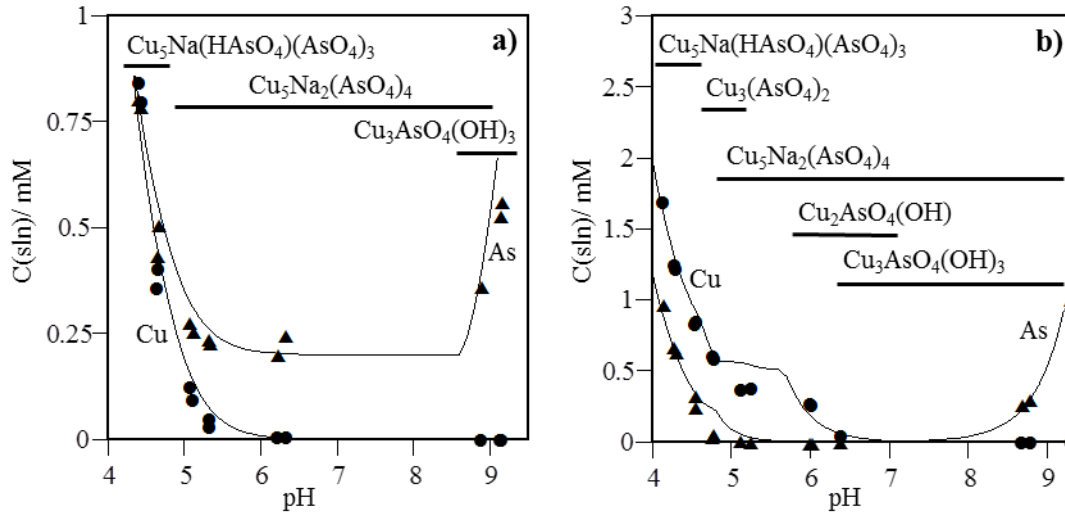


Figure 7.1. Concentration of copper and arsenate in solution as a function of pH. Symbols represent experimental data, (●) denotes copper (▲) denotes arsenate, and thin solid lines represent calculated values according to the proposed model. Bold lines indicate the pH interval where the different solid phases are stable. The copper to arsenate ratio (Cu(tc)/As(tc)) is in a) 1/1 and in b) 3/2.

The presence of  $\text{Na}^+$  in two of the copper(II) arsenates phases obtained has not to our knowledge been reported previously in the literature. Although not reported as minerals, these phases may precipitate to significant amounts in natural environments containing high sodium concentrations (mM concentrations).

A predominance area diagram, showing stability fields for copper(II) arsenate phases as a function of pNa and pH is presented in Figure 7.2. The Cu(tc)/As(tc) is here 1/1.

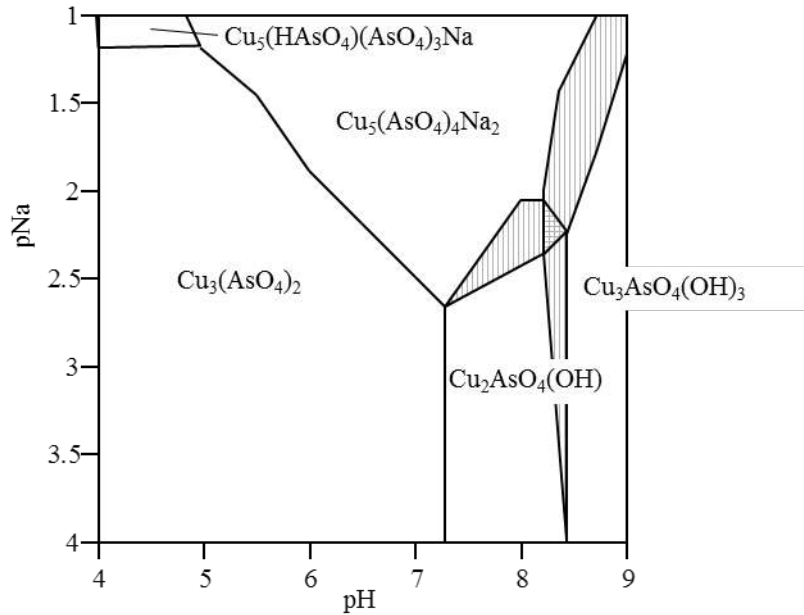


Figure 7.2. Predominance area diagram for copper(II) arsenates as a function of pNa and pH. Cu(tc)/As(tc) 1 mM/ 1 mM. Shaded areas show fields with two or three co-existing solid phases.

The solubility of copper(II) arsenates with different Cu(tc) to As(tc) ratios has been calculated according to the proposed model (Figure 7.3). Cu(sln) has solubility minima at pH 8-9 and the solubility,  $\log\text{Cu(sln)}$ , varies between -6 and -7 depending on Cu(tc) to As(tc) ratio. As(sln) has a minima at pH 6-7 and the solubility,  $\log\text{As(sln)}$ , varies between -3.5 and -7.0. This means that even very low concentrations, on the  $\mu\text{M}$  scale, can result in precipitation. The solubility pattern seen in Figure 7.3 can be explained by the Cu(tc) to As(tc) ratios of the solid phases formed, (c. f. Figure 7.2). For example, the increase in arsenate solubility at  $\text{pH} > 7$  (in ratios 1, 1.25 and 2), can be explained by the formation of  $\text{Cu}_3(\text{AsO}_4)(\text{OH})_3(\text{s})$  which has the highest Cu(tc) to As(tc) ratio.

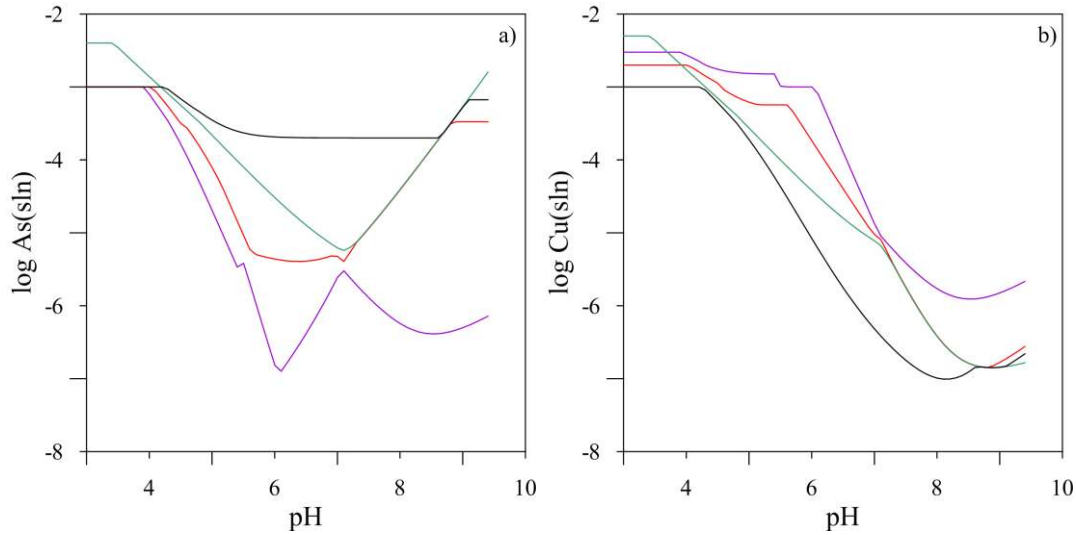


Figure 7.3. The solubility of a) arsenate and b) copper as a function of pH. The black curve represent Cu(tc)/ As(tc) = 1, green = 1.25, red = 2 and purple = 3, respectively. The total concentration of Cu(II) and arsenate is 1 mM ( $I = 0$  M).

## 7.2. Complexation of Arsenate and Copper(II) at the Goethite/ Water Interface

### 7.2.1. Arsenate Complexation

When modelling the adsorption of arsenate to the goethite surface, the objective was to design a simplified model with as few parameters as possible. Besides a determination of the formation constants the approach was to optimise the charge distribution for each stoichiometry to give a mean value of the possible locations of the proton. The model consists of two species with the stoichiometries 1:1:1:1 and 2:1:1:1 for the components  $H^+$ :  $HAsO_4^{2-}$ :  $=FeOH^{0.5-}$ :  $=Fe_3O^{0.5-}$ . These stoichiometries represent the average composition of un-, singly- and doubly- protonated arsenate ions (denoted  $S_{1As}$  and  $S_{2As}$  below) and the following formation constants and charge distributions were obtained:

	$lg\beta_{intr}$	$Q_0; Q_\beta$
$S_{1As} (\equiv FeOAsO_3H; \equiv Fe_3O)^{2-} /$ $(\equiv FeOAsO_3; \equiv Fe_3OH)^{2-}$	$18.71 \pm 0.02$	$-0.68; -1.32$
$S_{2As} (\equiv FeOAsO_3H_2; \equiv Fe_3O)^{1-} /$ $(\equiv FeOAsO_3H; \equiv Fe_3OH)^{1-}$	$24.00 \pm 0.01$	$-0.54; -0.46$

The distribution of the two different surface species as a function of pH is presented in Figure 7.4. The more acidic complex(es),  $(\equiv FeOAsO_3H_2; \equiv Fe_3O)^{1-} / (\equiv FeOAsO_3H; \equiv Fe_3OH)^{1-}$ , is dominating at  $pH < 6$  and the singly-/un-protonated complex(es),  $(\equiv FeOAsO_3H; \equiv Fe_3O)^{2-} / (\equiv FeOAsO_3; \equiv Fe_3OH)^{2-}$ , dominates at  $pH > 6$ . The charge distribution for  $S_{1As}$ , with  $-0.68$  of the charge in the 0-plane, implies that the proton in the hydrogen bond is located close to the adsorbed arsenate ion and in the case of  $S_{2As}$ , the



proton is located in the middle between the arsenate and the neighbouring site (See section 5.1.2 and 7.3 for a more detailed discussion about charge distribution according to Pauling's valance bond theory).

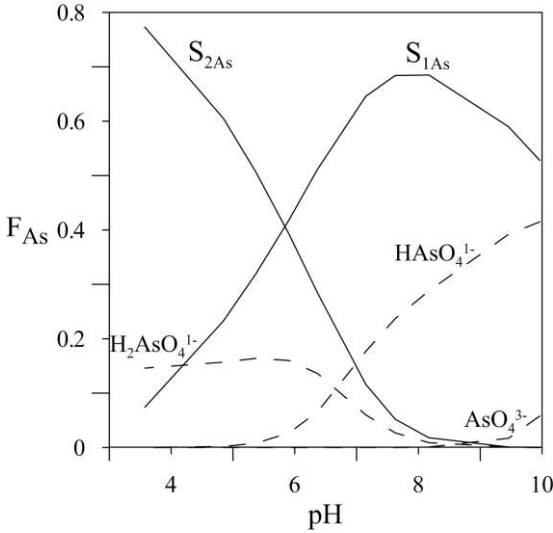


Figure 7.4. The distribution of arsenate at the goethite surface as a function of pH. Total concentration of arsenate is  $2.85 \mu\text{mol}/\text{m}^2$ .  $F_{\text{As}}$  is the fraction of total As. The different complexes are for simplicity presented with  $S_{X\text{As}}$  where  $S_{2\text{As}}$  represents  $(\equiv\text{FeOAsO}_3\text{H}_2; \equiv\text{Fe}_3\text{O})^{1-} / (\equiv\text{FeOAsO}_3\text{H}; \equiv\text{Fe}_3\text{OH})^{1-}$  and  $S_{1\text{As}}$  represents  $(\equiv\text{FeOAsO}_3; \equiv\text{Fe}_3\text{OH})^{2-} / (\equiv\text{FeOAsO}_3\text{H}; \equiv\text{Fe}_3\text{O})^{2-}$ .

### 7.2.2. Copper(II) Complexation

The adsorption of copper(II) at the goethite surface is modelled with four bidentate bridging inner sphere complexes. The set of complexes and the charge distribution are based on the model presented by Weng et al. [20]. A modification of the model presented here is that the bidentate complexes are coordinated to one singly and one triply coordinated surface site, as proposed by Hiemstra [21].

The formation constants ( $\lg\beta_{\text{intr}}$ ) and the charge distribution ( $Q_0; Q_\beta$ ) for the complexes are:

	$\lg\beta_{\text{intr}}$	$Q_0; Q_\beta$
$S_{1\text{Cu}} \equiv(\text{Fe}_3\text{OFeOH})\text{Cu}^{1+}$	$12.12 \pm 0.02$	-0.1; 1.1
$S_{2\text{Cu}} \equiv(\text{Fe}_3\text{OFeOH})\text{Cu}(\text{OH})^0$	$5.49 \pm 0.01$	-0.1; 0.1
$S_{3\text{Cu}} \equiv(\text{Fe}_3\text{OFeOH})\text{Cu}_2(\text{OH})_2^{1+}$	$5.63 \pm 0.02$	-0.1; 1.1
$S_{4\text{Cu}} \equiv(\text{Fe}_3\text{OFeOH})\text{Cu}_2(\text{OH})_3^0$	$-2.79 \pm 0.02$	-0.1; 0.1

To illustrate the relative importance of the different copper(II) surface complexes as a function of pH a distribution diagram has been constructed, representing a case with high surface coverage of copper(II), (Figure 7.5). Besides the bidentate, binuclear complex  $\equiv(\text{Fe}_3\text{OFeOH})\text{Cu}_2(\text{OH})_2^{1+}$ , the two monomeric copper(II) species are predominant over the whole pH range at the concentrations studied. At  $\text{pH} > 5$  the hydrolysed species are

dominating. Calculations at different copper(II) to goethite ratios show that dimeric species become more significant at higher total copper(II) concentrations and is dominating at  $\text{pH} \approx 5$  at total copper(II) concentrations  $> 2.5 \mu\text{mol}/\text{m}^2$ .

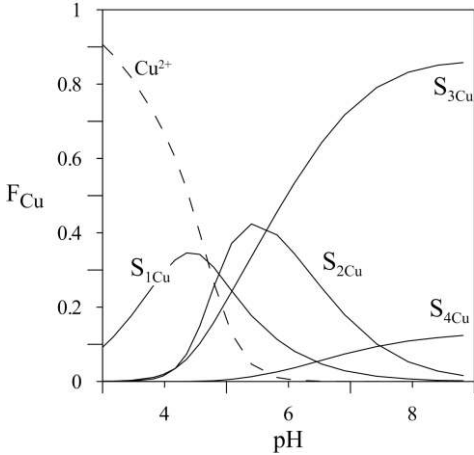


Figure 7.5. The distribution of copper at the goethite surface as a function of pH. Total concentration of copper(II) is  $2.81 \mu\text{mol}/\text{m}^2$ .  $F_{\text{Cu}}$  is the fraction of total Cu. The different complexes are for simplicity presented with  $S_{\text{XCu}}$  where  $S_{1\text{Cu}}$ ,  $S_{2\text{Cu}}$ ,  $S_{3\text{Cu}}$  and  $S_{4\text{Cu}}$  represents  $\equiv(\text{Fe}_3\text{OFeOH})\text{Cu}^{1+}$ ,  $\equiv(\text{Fe}_3\text{OFeOH})\text{Cu}(\text{OH})^0$ ,  $\equiv(\text{Fe}_3\text{OFeOH})\text{Cu}_2(\text{OH})_2^{1+}$  and  $\equiv(\text{Fe}_3\text{OFeOH})\text{Cu}_2(\text{OH})_3^0$  respectively.

### 7.2.3. Arsenate-Copper(II) Complexation

The basis of the model for the ternary system, arsenate-copper-goethite, is a combination of the copper(II)-goethite model (section 7.2.2) and the arsenate-goethite model with two surface complexes with optimized charge distribution (section 7.2.1). The adsorption of the individual ions could however not fully be predicted by the combined model from the two-component systems. The possibility of precipitation of solid copper(II)-arsenate phases was considered, but there was no indication of the formation of solids reported by Nelson et al. [4]. An alternate explanation for the enhanced adsorption observed is the formation of ternary surface complexes. The search for the set of surface complexes best describing experimental data included ternary surface complexes arranged in the order surface-metal-ligand (type A) and surface-ligand-metal (type B). In fact, the resulting model consists of one complex of each type. The charge distribution of the ternary complexes was set to be the same as for the corresponding complex in the binary system.

The final model includes the following formation constants ( $\lg\beta_{\text{intr}}$ ) and charge distributions ( $Q_0$ ;  $Q_\beta$ ):

	$\lg\beta_{\text{intr}}$	$Q_0$ ; $Q_\beta$
$S_{7\text{CuAs}} \equiv \text{FeOAsO}_3\text{Cu}^{0.5-}$	$13.42 \pm 0.08$	$-0.25$ ; $-0.25$
$S_{8\text{CuAs}} \equiv (\text{Fe}_3\text{OFeOH})\text{Cu}_2(\text{OH})_2\text{HAsO}_4^{1-}$	$13.15 \pm 0.12$	$-0.1$ ; $-0.9$

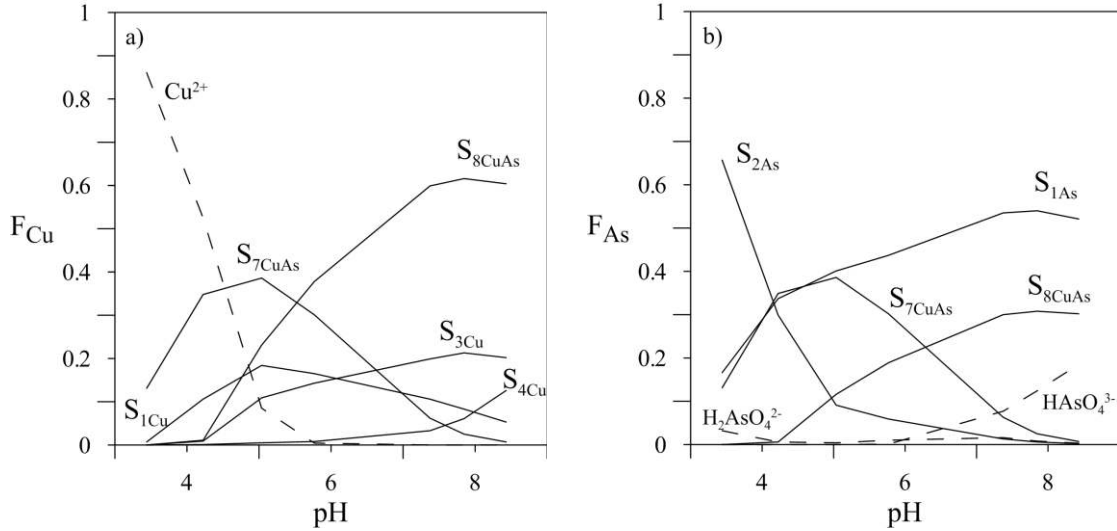


Figure 7.6. The distribution of copper(II) and arsenate at the goethite surface as a function of pH. Total concentration of arsenate and copper(II) is  $2.57 \mu\text{mol}/\text{m}^2$ .  $F_{\text{Cu}}$  and  $F_{\text{As}}$  is the fraction of total Cu and As respectively. The different complexes are presented as stoichiometries where  $S_{1\text{Cu}}$ ,  $S_{3\text{Cu}}$ ,  $S_{4\text{Cu}}$ ,  $S_{2\text{As}}$ ,  $S_{1\text{As}}$ ,  $S_{7\text{CuAs}}$  and  $S_{8\text{CuAs}}$  represents  $\equiv(\text{Fe}_3\text{OFeOH})\text{Cu}^{1+}$ ,  $\equiv(\text{Fe}_3\text{OFeOH})\text{Cu}_2(\text{OH})_2^{1+}$ ,  $\equiv(\text{Fe}_3\text{OFeOH})\text{Cu}_2(\text{OH})_3^0$ ,  $(\equiv\text{FeOAsO}_3\text{H}_2; \equiv\text{Fe}_3\text{O})^{1-} / (\equiv\text{FeOAsO}_3\text{H}; \equiv\text{Fe}_3\text{OH})^{1-}$ ,  $(\equiv\text{FeOAsO}_3; \equiv\text{Fe}_3\text{OH})^{2-} / (\equiv\text{FeOAsO}_3\text{H}; \equiv\text{Fe}_3\text{O})^{2-}$ ,  $\equiv\text{FeOAsO}_3\text{Cu}^{0.5-}$  and  $\equiv(\text{Fe}_3\text{OFeOH})\text{Cu}_2(\text{OH})_2\text{HAsO}_4^{1-}$  respectively.

By applying the present surface complexation model together with the precipitation model some interesting observations were made. Stability fields of the different arsenate–copper(II) precipitates as well as surface and solution speciation can be calculated. Furthermore, solubility curves as a function of pH with respect to As(V) and Cu(II) can be obtained.

Precipitation of copper(II) arsenates can be expected to form at  $\text{pH} > 4$  and at total solid concentration  $< 3 \text{ g}/\text{L}$ , i.e. at a total concentration of both copper(II) and arsenate equivalent to  $6.5 \mu\text{mol}/\text{m}^2$ , if the concentration of  $\text{Na}^+$  is high (Figure 7.7). In the case of low  $\text{Na}^+$  concentration, precipitation can be expected to form at a slightly higher solid concentration (Figure 7.8).

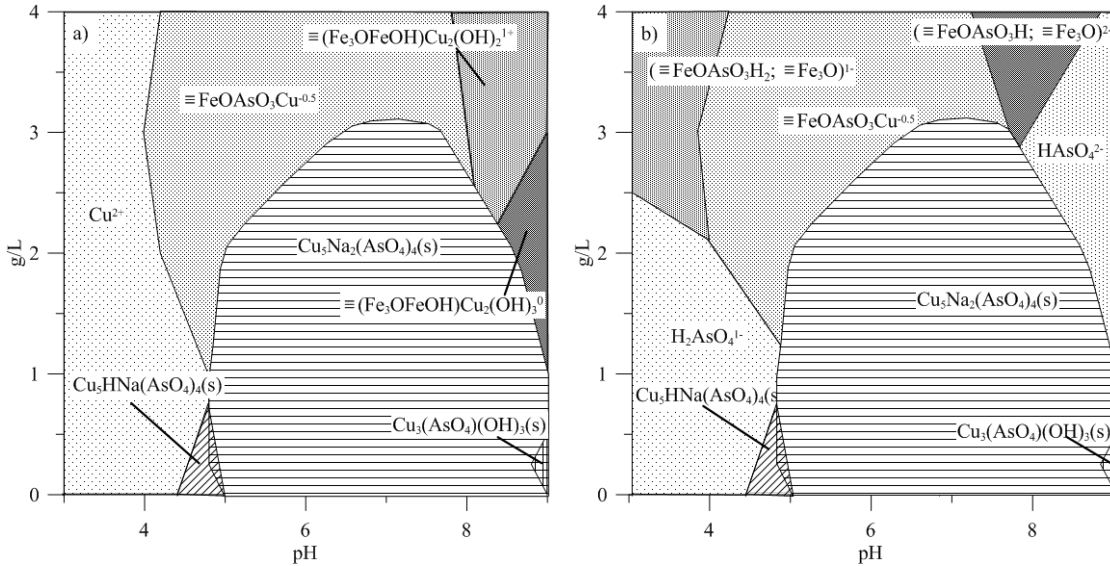


Figure 7.7. Stability area diagram for solid copper(II) arsenates and a) dominating copper(II) surface complex and b) dominating arsenate surface complex, as a function of solid concentration (g/L) and pH. The total concentration of Copper (II) and arsenate is 1 mM and the  $\text{Na}^+$  total concentration is 100 mM.

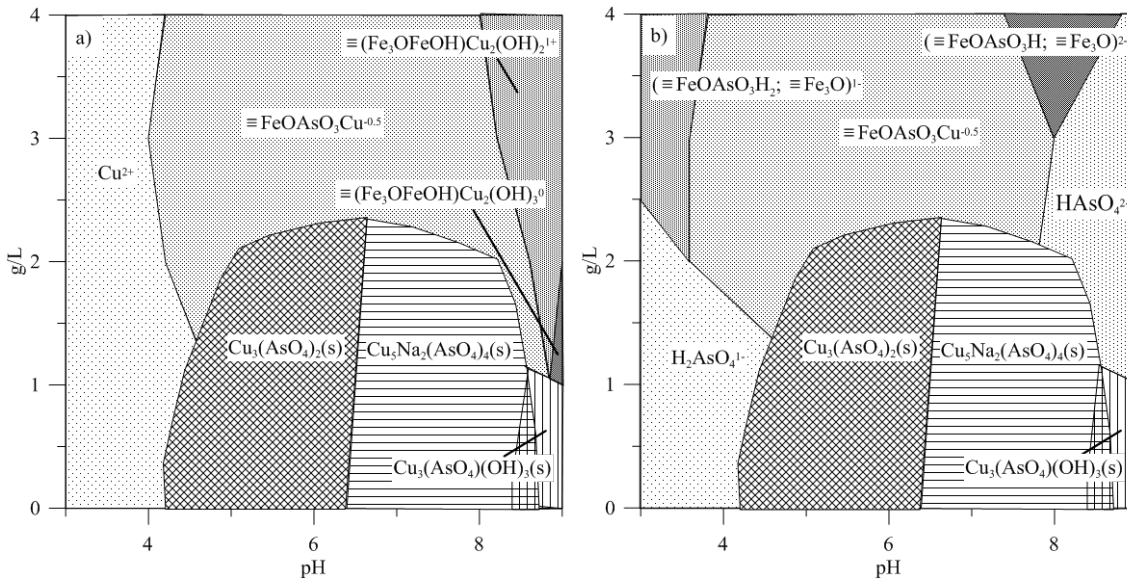


Figure 7.8. Stability area diagram for solid copper(II) arsenates and a) dominating copper(II) surface complex and b) dominating arsenate surface complex, as a function of solid concentration (g/L) and pH. The total concentration of Copper (II) and arsenate is 1 mM and the  $\text{Na}^+$  total concentration is 100 mM.

The solubility of copper(II) decreases with increasing pH, at the higher solid concentrations. This can be explained by increasing adsorption with increasing pH, but even in the case of very low or zero concentration of solids the concentration of copper(II) in solution is less than  $1 \mu\text{mol/L}$  at  $\text{pH} > 6$  due to precipitation of solid copper(II) arsenates, (c. f. Figure 7.7a).

The solubility of arsenate shows a different solubility pattern than that of copper(II). In absence of goethite (I in Figure 7.9b) the solubility of arsenate decreases with increasing pH due to precipitation of copper(II) arsenates (Figure 7.7b). With 2 g/l of goethite (II in Figure 7.9b) arsenate forms surface complexes at low pH and shows minimum solubility at pH 6 due to precipitation. At higher pH the precipitate is dissolved due to the strong affinity between the copper(II) ions and the goethite surface, and the arsenate ions are released into the solution. The same shape of the solubility curve can be seen with 4 g/l of goethite but here no precipitation is formed, only surface complexes. At high surface concentration (IV in Figure 7.9b) the solubility is only dependent on adsorption.

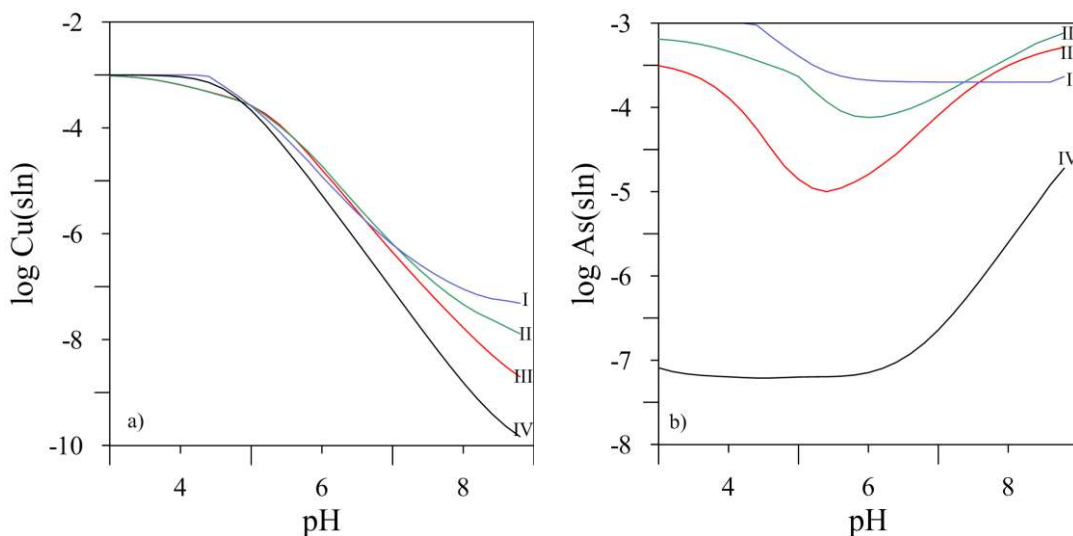


Figure 7.9. The solubility of a) copper and b) arsenate as a function of pH. The different curves represent different solid concentrations (g/l), I) 0, II) 2, III) 4 and IV) 10 g/l. The total concentration of Cu(II) and arsenate is 1 mM ( $I=0.1$  M).

### 7.3. Complexation of Monomethyl Phosphate, Phosphate and Arsenate at the Goethite/ Water Interface

When modelling adsorption of arsenate, phosphate and monomethyl phosphate at the goethite surface, the strategy of the modelling was to find a model that best described the macroscopic data and also was in agreement with the detailed spectroscopic result presented by Loring et al., [30] and Persson et al. [6], i.e. monodentate surface complexes stabilized by hydrogen bonding to neighbouring surface sites.

One of the challenges when constructing a model in agreement with the overall spectroscopic evidence is that two, or three, of the suggested surface complexes have the same stoichiometry but different location of the proton in the hydrogen bond. In one case the proton is assumed to be located at the ligand and in the other case the proton is assumed to be located closer to the neighbouring surface site. There is also the possibility of a transition where the proton is located somewhere between the two extremes.

Previously, surface speciation of arsenate to goethite was given with a simplified model involving only two surface species (section 7.2.1, [48]). However, these species are to be regarded as representing the average stability and the average charge distribution of the following surface isomers ( $\equiv\text{FeOAsO}_3\text{H}$ ;  $\equiv\text{Fe}_3\text{O}$ )<sup>2-</sup>/ $(\equiv\text{FeOAsO}_3$ ;  $\equiv\text{Fe}_3\text{OH})$ <sup>2-</sup> and ( $\equiv\text{FeOAsO}_3\text{H}_2$ ;  $\equiv\text{Fe}_3\text{O}$ )<sup>1-</sup>/ $(\equiv\text{FeOAsO}_3\text{H}$ ;  $\equiv\text{Fe}_3\text{OH})$ <sup>1-</sup> respectively.

The model with optimised charge distribution describes the proton data and the adsorption data very well but the spectroscopic information tells us that the picture is even more complicated than that. A different approach was used when modelling the monomethyl phosphate-goethite system in Paper III and the arsenate-and phosphate-goethite systems in Paper IV. Here, the charge distribution was used to separate complexes with the same stoichiometry but with different hydrogen bonding characteristics.

Applying Pauling's valance bond theory for the charge distribution, a complex with the proton located close to the ligand would have a  $Q_0$  charge of -0.75 and a complex with the proton at the neighbouring site would have a  $Q_0$  of 0.25. This approach gives six possible surface species in the case of arsenate and phosphate, Figure 7.10. By replacing the proton of the top hydroxyl group with a methyl group, three species are possible to form in the methyl phosphate system. This Figure does not show possible isomers where the proton is in transition between the ligand and the neighbouring site.

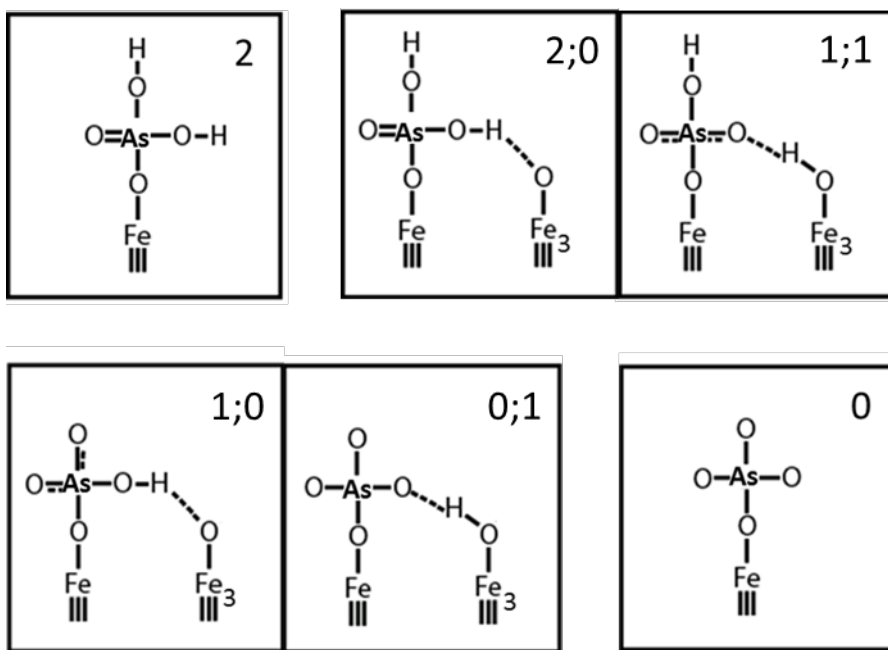


Figure 7.10. Cartoons showing possible stoichiometries and protonation modes of monodentate arsenate (phosphate)-goethite complexes hydrogen bonded to a neighboring surface site. Inset figures denote the number of protons bonded to the arsenate (phosphate) anion and the neighboring surface site.

### 7.3.1. Complexation of Monomethyl Phosphate

In the case of the adsorption of monomethyl phosphate to the goethite surface, both proton data, adsorption data and spectroscopic information was available (Paper III). The spectroscopic information is both qualitative and semi quantitative, Figure 7.11a.

The spectroscopic data conveys that the model should contain three monodentate inner sphere surface isomers stabilized by hydrogen bonding to a neighbouring surface site, all having the same overall stoichiometry but with different location of the proton in the hydrogen bond; one singly protonated complex hydrogen bonded to a unprotonated neighbouring site dominating at pH <6, one complex where the proton is located between the ligand and the neighbouring site dominating at pH 6-8 and one unprotonated surface complex hydrogen bonded to a protonated neighbouring surface site dominating at pH >8

Applying Pauling's bond valance theory to separate between surface isomers gives that a complex with the proton located at the monomethyl phosphate ion would have a  $Q_0$  charge of -0.75 and a complex with the proton at the neighbouring site would have a  $Q_0$  value of 0.25. For the complex where the proton is located somewhere between the two extremes, the best fit to experimental data was obtained with the charge in the 0-plane set to be zero. The complexes are for simplicity labelled according to number of protons bonded to the monomethyl phosphate anion and the neighbouring surface site.

The formation constants ( $\lg\beta_{\text{intr}}$ ) and the charge distribution ( $Q_0$ ;  $Q_\beta$ ) for the monomethyl phosphate-goethite surface complexes are:

	$\lg\beta_{\text{intr}}$	$Q_0$ ; $Q_\beta$
1;0 ( $\equiv\text{FeOPO}_3\text{HCH}_3$ ; $\equiv\text{Fe}_3\text{O}$ ) <sup>1-</sup>	21.5	-0.75; -0.25
0.3;0.7 ( $\equiv\text{FeOPO}_3\text{H}_{0.3}\text{CH}_3$ ; $\equiv\text{Fe}_3\text{OH}_{0.7}$ ) <sup>1-</sup>	23.9	0.0; -1.0
0;1 ( $\equiv\text{FeOPO}_3\text{CH}_3$ ; $\equiv\text{Fe}_3\text{OH}$ ) <sup>1-</sup>	24.2	0.25; -1.25

The distribution of monomethyl phosphate in solution and at the goethite surface was calculated applying the proposed model, Figure 7.11b. At pH < 5 the dominating complex is 1;0 for which MMP acts as a donor group in the hydrogen bond. In this pH region both 0.3;0.7 and 0;1 co-exist with 1;0, but at significantly lower fractions. With increasing pH the importance of 0.3;0.7 and 0;1 increases. At pH > 8.7 the major part of MMP exists as free unprotonated MMP in solution. This species distribution is in very good agreement with the ATR-FTIR data (c.f. Figure 7.11)

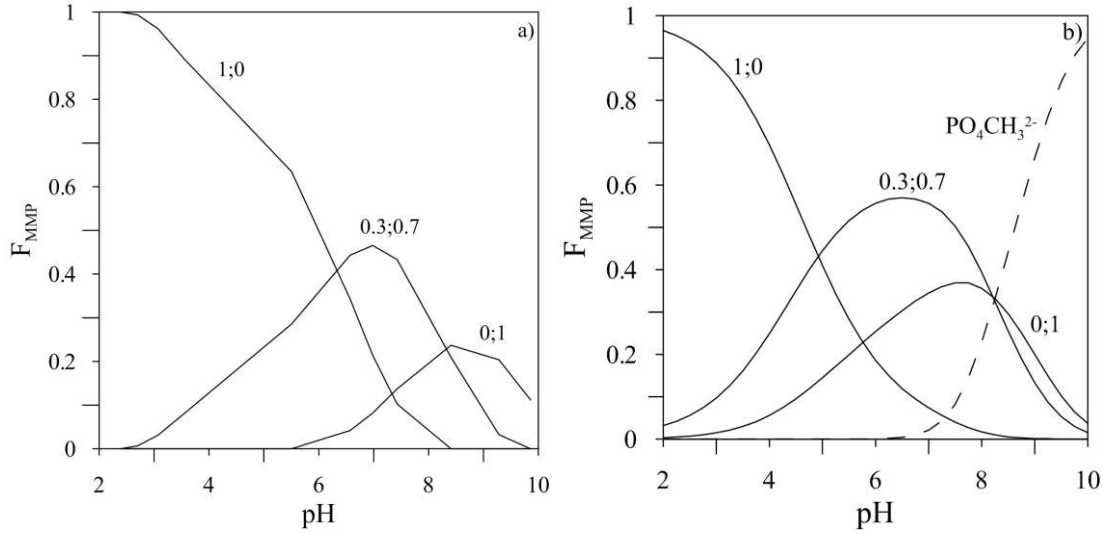


Figure 7.11. Distribution diagram for monomethyl phosphate in solution and at the water-goethite interface, a) from the multivariate curve resolution analysis of the infrared spectra b) according to the proposed model. The total concentration of monomethyl phosphate is  $0.81 \mu\text{mol}/\text{m}^2$ . F is the fraction of total concentration of monomethyl phosphate.

### 7.3.2. Complexation of Phosphate

Phosphate was assumed to adsorb on the goethite surface as illustrated in Figure 7.10, and all the six possible monodentate surface complexes where the phosphate atom is hydrogen bonded to a neighbouring surface site were included and the charge distribution was kept fixed according to Pauling's bond valence theory. The following results were obtained:

		$\lg\beta_{\text{intr}}$	$Q_0; Q_\beta$
0	$\equiv\text{FeOPO}_3^{2.5-}$	$7.61 \pm 0.03$	$-0.25; -2.25$
0,1	$(\equiv\text{FeOPO}_3; \equiv\text{Fe}_3\text{OH})^{2-}$	$20.51 \pm 0.02$	$0.25; -2.25$
1;0	$(\equiv\text{FeOPO}_3\text{H}; \equiv\text{Fe}_3\text{O})^{2-}$	$19.59 \pm 0.01$	$-0.75; -1.25$
1;1	$(\equiv\text{FeOPO}_3\text{H}; \equiv\text{Fe}_3\text{OH})^{1-}$	$26.41 \pm 0.02$	$0.25; -1.25$
2;0	$(\equiv\text{FeOPO}_3\text{H}_2; \equiv\text{Fe}_3\text{O})^{1-}$	$23.58 \pm 0.02$	$-0.75; -0.25$
2	$\equiv\text{FeOPO}_3\text{H}_2^{0.5-}$	$19.59 \pm 0.04$	$-0.25; -0.25$

The experimental results and the results from calculations using the model are presented in Figure 7.12 and Figure 7.13.



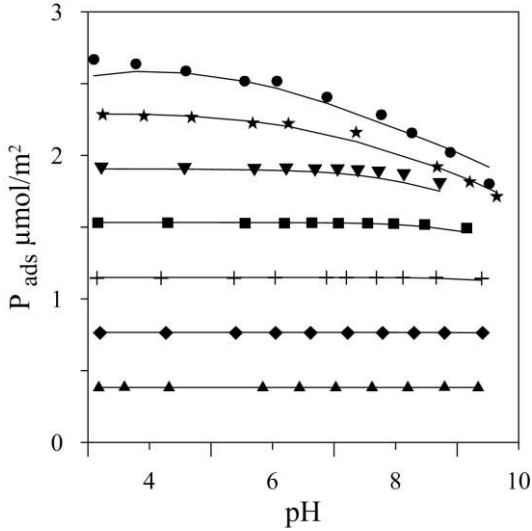


Figure 7.12. Adsorption of phosphate as a function of pH. Symbols represent experimental data and solid lines denote values calculated according to the model with six complexes. Total concentration of phosphate: ▲ 0.38, ◆ 0.77, + 1.15, ■ 1.53, ▼ 1.91, ★ 2.30 and ● 3.07  $\mu\text{mol}/\text{m}^2$ .

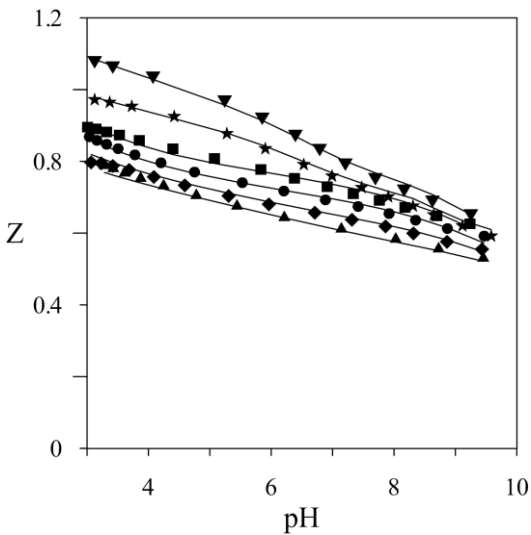


Figure 7.13. Z as a function of pH. Symbols represent experimental data and solid lines denote values calculated according to the model with six complexes. Total concentration of phosphate: ▲ 0.38, ◆ 0.77, ● 1.15, ■ 1.54, ★ 2.30 and ▼ 3.07  $\mu\text{mol}/\text{m}^2$ .

The surface speciation with respect to adsorbed phosphate is illustrated in Figure 7.14. Predominating species, in the pH range studied, are  $(\equiv\text{FeOPO}_3\text{H}_2; \equiv\text{Fe}_3\text{O})^{1-}$  and  $(\equiv\text{FeOPO}_3\text{H}; \equiv\text{Fe}_3\text{O})^{2-}$  (2;0 and 1;0) in which phosphate acts as a hydrogen bond donor. The protonation constant for the complex  $(\equiv\text{FeOPO}_3\text{H}; \equiv\text{Fe}_3\text{O})^{2-}$  (1;0) to give  $(\equiv\text{FeOPO}_3\text{H}_2; \equiv\text{Fe}_3\text{O})^{1-}$  (2;0) is approximately 2.5 at low coverage and 5 at high coverage (Figure 7.14a and b). This difference reflects the impact of surface charge on the formation constants. Furthermore, the protonation constant for  $\text{H}_2\text{PO}_4^-$  in solution is 2.15, which means that phosphate adsorbed to goethite has a higher affinity for protons than

phosphate in aqueous solution. This can (partly) be explained by hydrogen bond stabilization.

Furthermore, the 0;1 species in which phosphate is a hydrogen bond acceptor is favoured by a low coverage and high pH values, whereas the 1;1 species is only formed at high coverage.

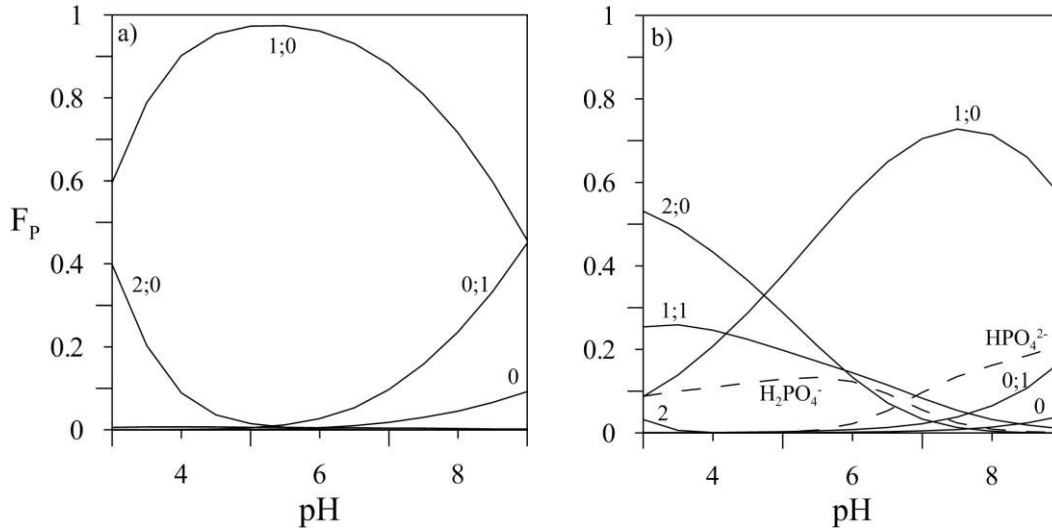


Figure 7.14. Distribution of phosphate species at total concentrations of a)  $0.6 \mu\text{mol/m}^2$  and b)  $2.7 \mu\text{mol/m}^2$ .  $F_p$  is the fraction of total P. The complexes are labelled according to Figure 7.10; 0 representing  $\equiv\text{FeOPO}_3^{2.5-}$ , 0;1 ( $\equiv\text{FeOPO}_3$ ;  $\equiv\text{Fe}_3\text{OH}$ ) $^{2-}$ , 1;0 ( $\equiv\text{FeOPO}_3\text{H}$ ;  $\equiv\text{Fe}_3\text{O}$ ) $^{2-}$ , 1;1 ( $\equiv\text{FeOPO}_3\text{H}$ ;  $\equiv\text{Fe}_3\text{OH}$ ) $^{1-}$ , 2;0 ( $\equiv\text{FeOPO}_3\text{H}_2$ ;  $\equiv\text{Fe}_3\text{O}$ ) $^{1-}$  and 2  $\equiv\text{FeOPO}_3\text{H}_2^{0.5-}$ .

### 7.3.3. Complexation of Arsenate

Two different approaches have been used when modelling the adsorption of arsenate at the goethite surface. In the first case, the charge distribution for each stoichiometry was allowed to vary to give a mean value of the possible locations of the proton (section 7.2.1, (Paper II) [48]).

In the second modelling, arsenate is assumed to adsorb at the goethite surface in the same way as phosphate (section 7.3.2), i.e. monodentate surface complexes hydrogen bonded to a neighbouring triply coordinated surface site. The model with six possible complexes and charge distribution according to Pauling's bond valence theory was applied to the arsenate-goethite system and the following results were obtained:

		$\lg\beta_{\text{intr}}$	$Q_0; Q_\beta$
0	$\equiv\text{FeOAsO}_3^{2.5-}$	$6.04 \pm 0.08$	-0.25; -2.25
0;1	( $\equiv\text{FeOAsO}_3$ ; $\equiv\text{Fe}_3\text{OH}$ ) $^{2-}$	$19.65 \pm 0.02$	0.25; -2.25
1;0	( $\equiv\text{FeOAsO}_3\text{H}$ ; $\equiv\text{Fe}_3\text{O}$ ) $^{2-}$	$18.57 \pm 0.02$	-0.75; -1.25
1;1	( $\equiv\text{FeOAsO}_3\text{H}$ ; $\equiv\text{Fe}_3\text{OH}$ ) $^{1-}$	$25.07 \pm 0.02$	0.25; -1.25
2;0	( $\equiv\text{FeOAsO}_3\text{H}_2$ ; $\equiv\text{Fe}_3\text{O}$ ) $^{1-}$	$23.46 \pm 0.04$	-0.75; -0.25
1	$\equiv\text{FeOAsO}_3\text{H}_2^{0.5-}$	$29.33 \pm 0.05$	-0.25; -0.25

The values of  $\lg\beta_{\text{intr}}$  are slightly lower in comparison to the phosphate system. This is in agreement with the general observation that phosphate anions form stronger complexes than arsenate anions. For the model with six possible surface complexes, two distribution diagrams, (Figure 7.15), have been constructed to illustrate the relative importance of the different surface complexes, one at low coverage ( $0.6 \mu\text{mol}/\text{m}^2$ ) where all arsenate are adsorbed and one at high coverage ( $2.7 \mu\text{mol}/\text{m}^2$ ).

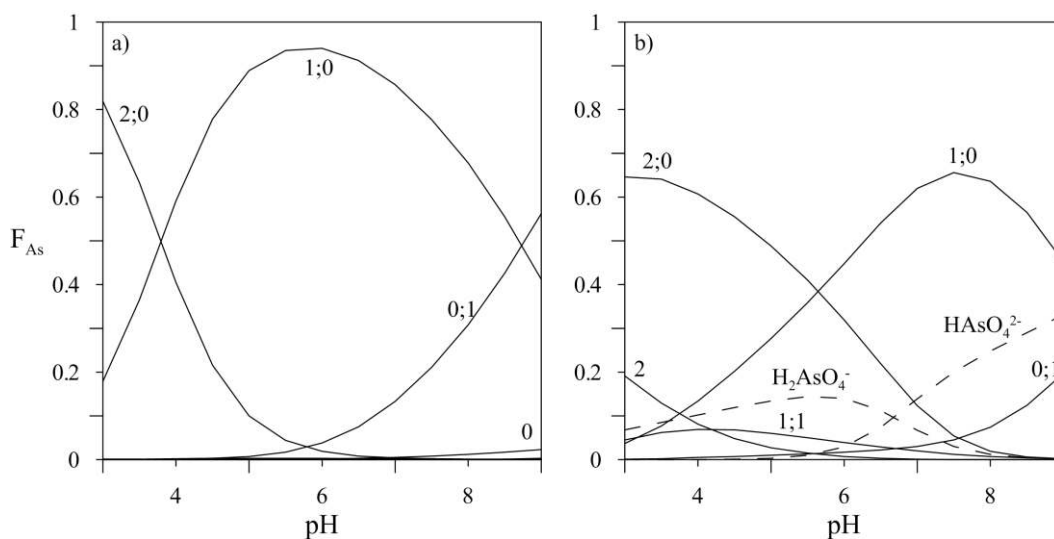


Figure 7.15. Distribution of arsenate at total concentrations of a)  $0.6 \mu\text{mol}/\text{m}^2$  and b)  $2.7 \mu\text{mol}/\text{m}^2$ .  $F_{\text{As}}$  is the fraction of total As. The complexes are labeled according to Figure 7.10; 0 representing  $\equiv\text{FeOAsO}_3^{2.5-}$ , 0;1 ( $\equiv\text{FeOAsO}_3$ ;  $\equiv\text{Fe}_3\text{OH}$ ) $^{2-}$ , 1;0 ( $\equiv\text{FeOAsO}_3\text{H}$ ;  $\equiv\text{Fe}_3\text{O}$ ) $^{2-}$ , 1;1 ( $\equiv\text{FeOAsO}_3\text{H}$ ;  $\equiv\text{Fe}_3\text{OH}$ ) $^{1-}$ , 2;0 ( $\equiv\text{FeOAsO}_3\text{H}_2$ ;  $\equiv\text{Fe}_3\text{O}$ ) $^{1-}$  and 2  $\equiv\text{FeOAsO}_3\text{H}_2^{0.5-}$ .

## 8. Summary and Conclusions

Based on data from potentiometric titrations, no significant formation of complexes containing  $\text{Cu}^{2+}$  and  $\text{AsO}_4^{3-}$  ions in aqueous solution could be detected, irrespective of pH and ratio in total concentrations of Cu(II) and As(V).

Mixing of  $\text{Cu}^{2+}$  and  $\text{HAsO}_4^{2-}$  solutions at different proportions in the range  $4 < \text{pH} < 9$  resulted in precipitation of solid phases of five different stoichiometric compositions. Precipitation occurred at pH above 4, at all copper to arsenate ratios. The solubility of the solid phases was lowest under neutral and weakly alkaline conditions.  $\text{Na}^+$  was found to be a component in two of the solid phases ( $\text{Cu}_5\text{Na}(\text{HAsO}_4)(\text{AsO}_4)_3$  and  $\text{Cu}_5\text{Na}_2(\text{AsO}_4)_4$ ), which were formed at all Cu(II) to As(V) ratios.

The adsorption of arsenate to the goethite surface was explained in the simplified model by introducing two different proton stoichiometries. Both stoichiometries represent monodentate inner-sphere arsenate groups and involve hydrogen bonding to a neighbouring triply coordinated oxide group. The refined charge distributions indicate that these stoichiometries represent the average charge of two (or more) surface species. The adsorption of copper(II) was described with four inner-sphere surface complexes, all involving two adjacent surface sites, one singly coordinated hydroxyl group and one triply coordinated oxide group. In the mixed system, the arsenate and copper(II) adsorption could not be predicted by applying the combined model from the two binary systems. A sensitivity analysis showed that the additional effects could not be explained by the formation of precipitates. Instead, two ternary copper- arsenate- goethite surface complexes were found to give a good fit. One of the ternary complexes is arranged in the order surface hydroxyl-copper-arsenate and the other surface hydroxyl-arsenate-copper.

The adsorption of arsenate or phosphate anions at the goethite/water interface is more complex than previously assumed, a great number of species seem to form. Several of these can be regarded as surface isomers. In the monomethyl phosphate system three isomers are formed with the difference being found in the location of the proton in the hydrogen bond, giving rise to different surface charge distributions. In the arsenate (and phosphate) systems the number of surface species is amounts to six *viz.*  $\equiv\text{FeOAsO}_3^{2.5-}$ ;  $(\equiv\text{FeOAsO}_3; \equiv\text{Fe}_3\text{OH})^{2-}$ ;  $(\equiv\text{FeOAsO}_3\text{H}; \equiv\text{Fe}_3\text{O})^{2-}$ ;  $(\equiv\text{FeOAsO}_3\text{H}; \equiv\text{Fe}_3\text{OH})^{1-}$ ;  $(\equiv\text{FeOAsO}_3\text{H}_2; \equiv\text{Fe}_3\text{O})^{1-}$  and  $\equiv\text{FeOAsO}_3\text{H}_2^{0.5-}$ . Two + two isomers are formed, but it seems likely that even more are formed also here as in the MMP system with three isomers for the same stoichiometry. However, more detailed spectroscopic data is needed before such interpretations can be made. Furthermore, the charge distribution of the different surface species in which not only the surface itself and the anions play a role, but also the location of the proton in the hydrogen bond, reveals the complexity of the electrical double layer.

Including precise spectroscopic data in the modelling results in a greater number of adjustable parameters but gives models with a more physical/chemical relevance and also a more detailed understanding of the complexity of the coordination chemistry of particle surfaces.

## 9. References

1. Reddy, K.R., et al., *Phosphorus retention in streams and wetlands: A review*. Critical reviews in Environmental Science and Technology, 1999(29): p. 83-146.
2. E.A., P. and C. F.E., *Soil microbiology and biochemistry*. 2 ed 1996, New York: Academic Press.
3. Smedley, P.L. and D.G. Kinniburgh, *A review of the source, behaviour and distribution of arsenic in natural waters*. Applied Geochemistry, 2002. 17(5): p. 517-568.
4. Nelson, H., et al., *Composition and solubility of precipitated copper(II) arsenates*. Applied Geochemistry, 2011. 26(5): p. 696-704.
5. Smith, R.M. and A.E. Martell, *Critical Stability Constants volume 4: Inorganic Complexes*, 1976, New York: Plenum Press.
6. Persson, P., et al., 2012. *Surface complexes of monomethyl phosphate stabilized by hydrogen bonding on goethite ( $\alpha$ -FeOOH) nanoparticles*. Submitted to Journal of Colloid and Interface Science, 2012.
7. Powell, K.J., et al., *Chemical speciation of environmentally significant metals with inorganic ligands - Part 2: The  $\text{Cu}^{2+}$ -OH, Cl,  $\text{CO}_3^{2-}$ ,  $\text{SO}_4^{2-}$ , and  $\text{PO}_4^{3-}$  systems - (IUPAC technical report)*. Pure and Applied Chemistry, 2007. 79(5): p. 895-950.
8. Marini, L. and M. Accornero, *Prediction of the thermodynamic properties of metal-arsenate and metal-arsenite aqueous complexes to high temperatures and pressures and some geological consequences*. Environmental Geology, 2007. 52(7): p. 1343-1363.
9. Lee, J.S. and J.O. Nriagu, *Stability constants for metal arsenates*. Environmental Chemistry, 2007. 4(2): p. 123-133.
10. Pettit, L.D. and K.J. Powell, *IUPAC Stability Constants Database*, 2009, IUPAC; Academic Software Otley, UK.
11. Magalhães, M.C.F., J.D.P. DeJesus, and P.A. Williams, *The Chemistry of Formation of Some Secondary Arsenate Minerals of Cu(II), Zn(II) and Pb(II)*. Mineralogical Magazine, 1988. 52(368): p. 679-690.
12. Chukhlantsev, V.G., *Solubility of several arsenates*. J. Inorg.Chem. USSR, 1956. 1: p. 1975-1982.
13. Schwertmann, U. and R.M. Taylor, *Minerals in soil environments*. Vol. Ch. 5. 1977, Madison, Wisconsin: Soil science society of America Inc.
14. Boily, J.F., et al., *Modeling proton binding at the goethite ( $\alpha$ -FeOOH)-water interface*. Colloids and Surfaces a-Physicochemical and Engineering Aspects, 2001. 179(1): p. 11-27.
15. Lützenkirchen, J., et al., *Protonation of different goethite surfaces - Unified models for  $\text{NaNO}_3$  and  $\text{NaCl}$  media*. Journal of Colloid and Interface Science, 2008. 317(1): p. 155-165.
16. M., L., *Aqueous Surface Chemistry of Goethite- Adsorption and desorption Reactions Involving Phosphate and Carboxylic Acids*, in *Department of Chemistry* 2009, Umeå University.
17. Bochatay, L., et al., *XAFS Study of Cu(II) at the Water-Goethite ( $\alpha$ -FeOOH) Interface*. J. Phys. IV France, 1997. 7: p. C2 819-820.

18. Robertson, A.P. and J.O. Leckie, *Acid/base, copper binding, and  $Cu^{2+}/H^+$  exchange properties of goethite, an experimental and modeling study*. Environmental Science & Technology, 1998. 32(17): p. 2519-2530.
19. Peacock, C.L. and D.M. Sherman, *Copper(II) sorption onto goethite, hematite and lepidocrocite: A surface complexation model based on ab initio molecular geometries and EXAFS spectroscopy*. Geochimica Et Cosmochimica Acta, 2004. 68(12): p. 2623-2637.
20. Weng, L.P., W.H. Van Riemsdijk, and T. Hiemstra,  *$Cu^{2+}$  and  $Ca^{2+}$  adsorption to goethite in the presence of fulvic acids*. Geochimica Et Cosmochimica Acta, 2008. 72(24): p. 5857-5870.
21. Hiemstra, T., *Surface complexation at mineral surfaces: Multisite and Charge Distribution approach*, in *Departement Bodemkwaliteit*, 2010, Wageningen University: Wageningen. p. 381.
22. Grafe, M., et al., *Arsenic speciation in multiple metal environments - I. Bulk-XAFS spectroscopy of model and mixed compounds*. Journal of Colloid and Interface Science, 2008. 320(1): p. 383-399.
23. Grafe, M., et al., *Copper and arsenate co-sorption at the mineral-water interfaces of goethite and jarosite*. Journal of Colloid and Interface Science, 2008. 322(2): p. 399-413.
24. Khaodhiar, S., et al., *Copper, chromium, and arsenic adsorption and equilibrium modeling in an iron-oxide-coated sand, background electrolyte system*. Water Air and Soil Pollution, 2000. 119(1-4): p. 105-120.
25. Waychunas, G.A., et al., *Surface-chemistry of ferrihydrite. 1. EXAFS studies of the geometry of coprecipitated and adsorbed arsenate*. Geochimica Et Cosmochimica Acta, 1993. 57(10): p. 2251-2269.
26. Fendorf, S., et al., *Arsenate and chromate retention mechanisms on goethite . 1. Surface structure*. Environmental Science & Technology, 1997. 31(2): p. 315-320.
27. Farquhar, M.L., et al., *Mechanisms of arsenic uptake from aqueous solution by interaction with goethite, lepidocrocite, mackinawite, and pyrite: An X-ray absorption spectroscopy study*. Environmental Science & Technology, 2002. 36(8): p. 1757-1762.
28. Sherman, D.M. and S.R. Randall, *Surface complexation of arsenic(V) to iron(III) (hydr)oxides: Structural mechanism from ab initio molecular geometries and EXAFS spectroscopy*. Geochimica Et Cosmochimica Acta, 2003. 67(22): p. 4223-4230.
29. Tejedor-Tejedor, M.I. and M.A. Anderson, *protonation of phosphate on the surface of goethite as studied by cir-ftir and electrophoretic mobility*. Langmuir, 1990. 6(3): p. 602-611.
30. Loring, J.S., et al., *Rethinking Arsenate Coordination at the Surface of Goethite*. Chemistry-a European Journal, 2009. 15(20): p. 5063-5072.
31. Stachowicz, M., T. Hiemstra, and W.H. van Riemsdijk, *Surface speciation of As(III) and As(V) in relation to charge distribution*. Journal of Colloid and Interface Science, 2006. 302(1): p. 62-75.
32. Fukushi, K. and D.A. Sverjensky, *A predictive model (ETLM) for arsenate adsorption and surface speciation on oxides consistent with spectroscopic and theoretical molecular evidence*. Geochimica Et Cosmochimica Acta, 2007. 71(15): p. 3717-3745.

33. Rahnemaie, R., T. Hiemstra, and W.H. van Riemsdijk, *Geometry, charge distribution, and surface speciation of phosphate on goethite*. Langmuir, 2007. 23(7): p. 3680-3689.
34. Goldberg, S., *Chemical modeling of arsenate adsorption on aluminum and iron-oxide minerals*. Soil Science Society of America Journal, 1986. 50(5): p. 1154-1157.
35. Manning, B.A. and S. Goldberg, *Modeling competitive adsorption of arsenate with phosphate and molybdate on oxide minerals*. Soil Science Society of America Journal, 1996. 60(1): p. 121-131.
36. Salazar-Camacho, C. and M. Villalobos, *Goethite surface reactivity: III. Unifying arsenate adsorption behavior through a variable crystal face - Site density model*. Geochimica Et Cosmochimica Acta, 2010. 74(8): p. 2257-2280.
37. Hiemstra, T., W.H. Vanriemsdijk, and G.H. Bolt, *Multisite proton adsorption modeling at the solid-solution interface of (hydr)oxides - A new approach. 1. Model description and evaluation of intrinsic reaction constants*. Journal of Colloid and Interface Science, 1989. 133(1): p. 91-104.
38. Ginstrup, O., *Experimental and Computational Methods for Studying Multicomponent Equilibria .2. Automated System for Precision Emf Titrations*. Chemical Instrumentation, 1972. 4(3): p. 141-155.
39. *Swedish Standard SS 02 81 27*. 1984.
40. Stumm, W. and J.J. Morgan, *Aquatic Chemistry, Chemical Equilibria and Rates in Natural Waters*. 3 th ed 1996, New York: John Wiley & Sons inc.
41. J, L., B. J-P, and S. S, *Current application of and future requirements for surface complexation models*. Current Topics in Colloid & Interface Science, 2002. 5: p. 157-190.
42. Hiemstra, T., J.C.M. Dewit, and W.H. Vanriemsdijk, *Multisite proton adsorption modeling at the solid-solution interface of (hydr)oxides - A new approach. 2. Applications to various important (hydr)oxides*. Journal of Colloid and Interface Science, 1989. 133(1): p. 105-117.
43. Pauling, L., J. Am. Chem. Soc., 1929. 51: p. 1010-1026.
44. Venema, P., et al., *Intrinsic proton affinity of reactive surface groups of metal (hydr)oxides: Application to iron (hydr)oxides*. Journal of Colloid and Interface Science, 1998. 198(2): p. 282-295.
45. Karlsson, M. and J. Lindgren, *WinSGW, a user interface for SolGasWater*, [www.winsgw.se](http://www.winsgw.se), 2006.
46. Eriksson, G., *An Algorithm for the computation of aqueous multicomponent, multiphase equilibriums*. Analytica Chimica Acta, 1979. 112(4): p. 375-383.
47. Davies, C.W., *Ion Association* 1962, London: Butterworth.
48. Nelson, H., S. Sjöberg, and L. Lövgren, *Surface complexation modeling of arsenate and copper adsorbed at the goethite/ water interface*. Submitted to Applied Geochemistry, 2012.



## Acknowledgements

Det är så många av er som läser det här som jag vill tacka, så många som har inspirerat, hjälpt, påverkat och berört mig. Ni har sett mig skratta, gråta och förbanna. Jag är så glad att jag har så fina människor omkring mig!

Lars och Staffan- kunde inte haft handledare som passat mig bättre! Ni har alltid sett till mitt bästa. Jag har kommit i första hand, vilket har lett till bra resultat i slutändan.

Per- även om du inte varit så inblandad i mitt arbete så har det varit trygt att veta att du finns där i bakgrunden. Lage- ditt stöd och din uppmuntran betyder så mycket. Ingegärd och Gun-Britt- allt som ni fixade och donade, ni är saknade. Gun- tackvare dig var det fantastiskt lätt och roligt att undervisa. Thomas- du är faktiskt en av anledningarna till att jag är här. Du undervisade på den första kurs jag läste i Umeå, en av de bästa jag läst. John- your enthusiasm and your discussions were really inspiring. Johannes- dina kunskaper om ytan var värdefulla.

Alla fina, nya och gamla, doktoander från avdelningen.

Malin, Rickard, Janice, Kristoffer, Andràs, Thomas, Åsa, Katarina, Caroline- ni är speciella.

Min älskade, älskade, älskade, älskade familj- ni är de finaste som finns, och viktigast av allt! Mamma Pappa Emma Lou Kitty Tobias Tyra- jag älskar er!